Chemistry–A European Journal

Supporting Information

Erythrose and Threose: Carbonyl Migrations, Epimerizations, Aldol, and Oxidative Fragmentation Reactions under Plausible Prebiotic Conditions

Ruiqin Yi,* Ryan Kern, Pamela Pollet, Huacan Lin, Ramanarayanan Krishnamurthy,* and Charles L. Liotta*

Supporting Information

Table of Contents: **Page**

1. General Methods

1.1 General considerations

All reactions were carried out in 18 MΩ water using a MilliQ purification system. All reagents were purchased from Sigma Aldrich, except for D-[1-^{13}C]-erythrose solution (0.096 M), D-[4-^{13}C]-erythrose solution (0.107 M), and D-[1-^{13}C]-threose solution (0.110 M), 20% ^{13}C-formaldehyde (8 M), which were purchased from Omicron Biochemicals, and used without further purification. The pH of all buffer solution was adjusted using minimal amounts of 37% HCl and 10 M NaOH.

1.2 NMR spectroscopy

NMR spectra were acquired on a Bruker (Billerica, MA, USA) Avance^{III} 500 MHz and AV-600 MHz NMR spectrometer (500 MHz for ^{1}H, 125 MHz for ^{13}C, and 600 MHz for ^{1}H, 151 MHz for ^{13}C). DMSO-d6 (in a sealed 1 mm capillary) and D_2O were used as the lock solvent. Carbon chemical shifts are reported in parts per million (ppm) constants on the δ scale and were typically referenced to the d6-DMSO signal (δ = 39.5 ppm) and D_2O. The peak intensity t for each signal was determined by integration of the ^{13}C NMR against d6-DMSO standard. Unless otherwise indicated, all NMR spectra were recorded at 40 °C, and analyzed using MestReNova (MestreLab Research, Santiago de Compostela, Spain).

1.3 Mass spectroscopy

Samples were diluted 2000× with water, mixed with H-resin to remove Na^+, and filtered prior to MS analysis. ESI quadrupole time-of-flight MS (ESI-QToF-MS) analysis was carried out by direct infusion at a flow rate of 0.2 mL min^{-1} using a Waters Xevo G2-XS QToF-MS operated in positive mode. Under positive mode ESI conditions, a voltage of 3.0 kV was applied to the stainless-steel electrospray ionizer. The TOF analyzer was set to sensitivity mode with a resolving power of 22,000, and the set *m/z* range of 50–600 was calibrated with sodium formate. The desolvation gas (nitrogen) was used at a flow rate of 300 L h^{-1}, and the source and desolvation temperatures were set to 80 °C and 100 °C, respectively.

2. General Procedures for carbonyl migration experiments

2.1 D-[1-^{13}C]-Erythrose

A 5 mL aqueous stock solution containing 1 M $NaHCO_3$ (0.42 g $NaHCO_3$, 5 mmol) was prepared and adjusted to pH 8.5. Then 420 μL of 96 mM D-[1-^{13}C]-erythrose stock solution was mixed with 80 μL of 1 M $NaHCO_3$ in a 1.5 mL Eppendorf tube to produce a 0.5 mL aqueous solution containing 80 mM D-[1-^{13}C]-erythrose and 160 mM $NaHCO_3$ buffered at pH 8.5. This solution was loaded into an NMR tube and NMR measurements were made at 25 °C (**Figure 2**).

2.1.1 Variable pH. A procedure similar to that of **2.1** was used to prepare the solutions for the pH studies shown in **Figure S1–S4**, except the solutions were prepared separately using the following stock buffers at the designated pH and heated at 40 °C.

1. 1 M CH_3COOK stock solution (5 mL, 0.49 g CH_3COOK, 5 mmol), pH 5, **Figure S1**.
2. 1 M NaH_2PO_4 stock solution (5 mL, 0.60 g NaH_2PO_4, 5 mmol), pH 7, **Figure S2**.
3. 1 M $NaHCO_3$ stock solution (5 mL, 0.49 g $NaHCO_3$, 5 mmol), pH 8.5, **Figure S3**.
4. 1 M $NaHCO_3$ stock solution (5 mL, 0.49 g $NaHCO_3$, 5 mmol), pH 10, **Figure S4**.

2.1.2 Variable buffer. A similar procedure to that of **2.1** was used to prepare the solutions for exploring the effect of base shown in **Figure S5**, **S6**, except the solutions were separately prepared using the following stock buffer at pH 7.

1. 3.8 M NaH_2PO_4 stock solution (5 mL, 2.28 g NaH_2PO_4, 19 mmol), pH 7, **Figure S5**.
2. 1 M sodium cacodylate stock solution (2 mL, 0.43 g sodium cacodylate trihydrate, 2 mmol), pH 7, **Figure S6**.

2.2 D-[4-^{13}C]-Erythrose

A 10 mL aqueous stock solution containing 1 M $NaHCO_3$ (0.84 g, 0.01 mol) was prepared and adjusted to pH 8.5. Then 374 μL of 107 mM D-[4-^{13}C]-erythrose stock solution was mixed with 126 μL of 1 M $NaHCO_3$ to produce a 0.5 mL aqueous solution containing 80 mM D-[4-^{13}C]-erythrose and 250 mM $NaHCO_3$ buffered at pH 8.5. This solution was loaded into an NMR tube and heated to 40 °C. (**Figure S7**).

2.3 D-[1-^{13}C]-Erythrose and D-[4-^{13}C]-Erythrose

A 10 mL aqueous stock solution containing 1 M $NaHCO_3$ (0.84 g, 0.01 mol) was prepared and adjusted to pH 8.5. Then 106 μL of 375 mM D-[1-^{13}C]-erythrose stock solution,187 μL of 107 mM D-[4-^{13}C]-erythrose stock solution and 127 μL H_2O were mixed with 80 μL of 1 M $NaHCO_3$ to produce a 0.5 mL aqueous solution containing 40 mM D-[4-^{13}C]-erythrose, 40 mM D-[1-^{13}C]-erythrose and 160 mM $NaHCO_3$ buffered at pH 8.5. This solution was loaded into an NMR tube and heated to 40 °C. (**Figure S8**).

2.4 D-[1-^{13}C]-Threose

A 10 mL aqueous stock solution containing 1 M $NaHCO_3$ (0.84 g, 0.01 mol) was prepared and adjusted to pH 8.5. Then 364 μL of 110 mM D-[1-^{13}C]-threose stock solution was mixed with 80 μL of 1 M $NaHCO_3$ and 56 μL of H_2O to produce a 0.5 mL aqueous solution containing 80 mM D-[1-^{13}C]-threose and 160 mM $NaHCO_3$ buffered at pH 8.5. This solution was loaded into an NMR tube and heated to 40 °C (**Figure S9**).

Effect of Oxygen. In order to investigate the influence of oxygen on the formation of formate, a procedure similar to **2.3** was used to prepare the solution except for employing a N_2 degassing process. (364 μL of 110 mM D-[1-^{13}C]-threose stock solution was mixed with 56 μL of H_2O, and then degassed by N_2 gas for 20 mins. The stock $NaHCO_3$ solution was also degassed by N_2 gas for 20 mins before mixing with the threose solution. The mixed solution was transferred into the NMR tube and degassed by N_2 gas for 2 mins and pH increased to 9 after degassing (**Figure S10**). A control experiment with an air-enrich process (the above solution in **2.3** was kept slowly bubbling with air when heating to 40 °C) was also carried out and the recorded ^{13}C and ^{1}H NMR spectra were shown in **Figure S11**, **S12**.

2.5 ^{13}C-Formaldehyde

0.31 μL of 20% ^{13}C-formaldehdye stock solution (8 M) was mixed with 80 μL of 1 M $NaHCO_3$ and 420 μL of H_2O to produce a 0.5 mL aqueous solution containing 5 mM ^{13}C-formaldehdye and 160 mM $NaHCO_3$ buffered at pH 8.5. This solution was loaded into an NMR tube and heated to 40 °C (**Figure S13**).

2.6 Aldol reaction of glycolaldehyde

To a vial containing 4 mL $NaHCO_3$ buffer (0.5 M or 1.0 M, pH = 8.5) or phosphate buffer (0.5 M, pH = 7.0), was added unlabeled glycolaldehyde (200 mM). The reactions were performed at room temperature in $NaHCO_3$ buffer or 40 °C in phosphate buffer. Progress of reactions were monitored by ^{1}H and ^{13}C NMR (**Figure S14–S17**).

3. NMR spectra

3.1 D-[1-^{13}C]-Erythrose

3.1.1 pH 5, 160 mM acetate, 40 °C

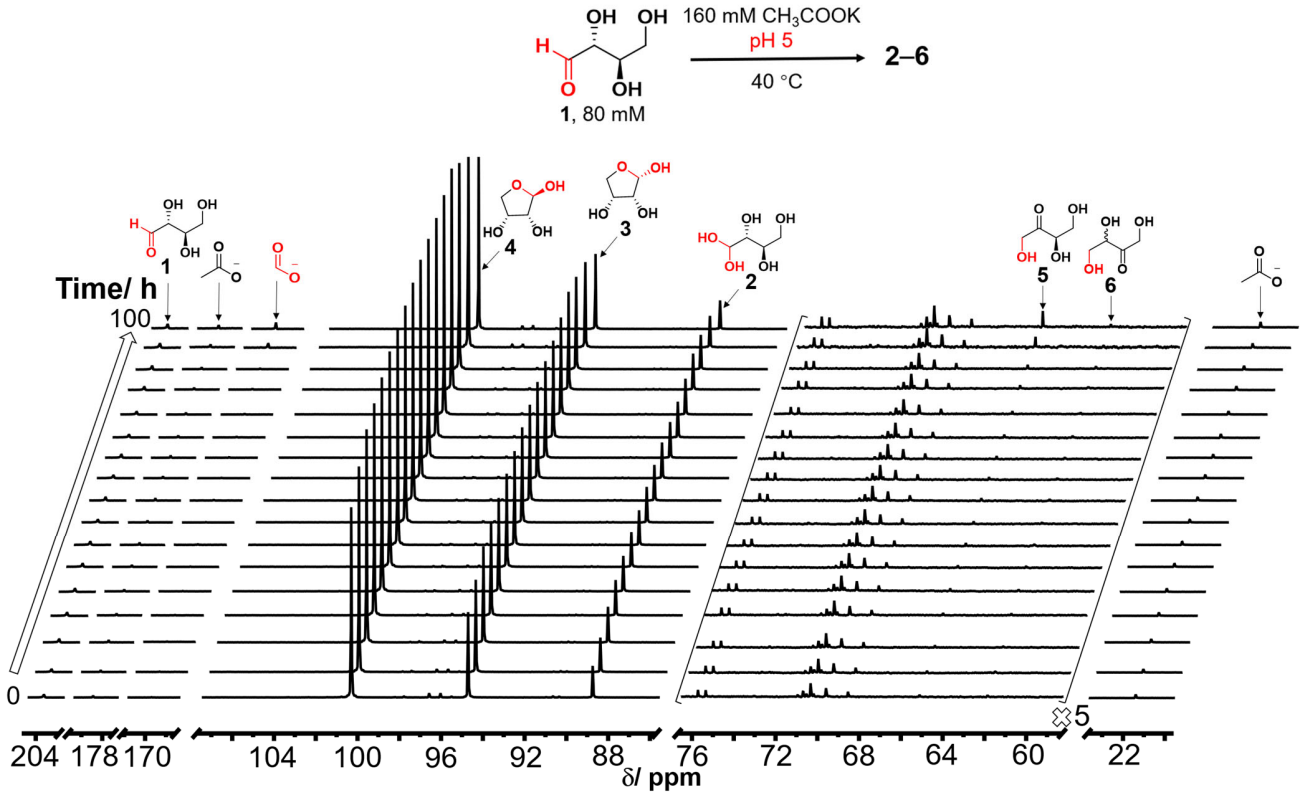

Figure S1. ^{13}C NMR spectra of 80 mM D-[1-^{13}C]-erythrose **1** with 160 mM acetate buffer at pH 5 at 40 °C over time. D-Erythrose (aldose **1**, hydrate **2** and cyclic ring **3**, **4**), D-erythrulose **5**, *rac*-erythrulose **6** were observed in these spectra over time and the peak intensities in each spectrum are recorded in **Table S2**. The rates of formation and disappearance of each species over a period of 100 hours is graphically displayed in **Figure S19**.

3.1.2 pH 7, 160 mM NaH_2PO_4, 40 °C

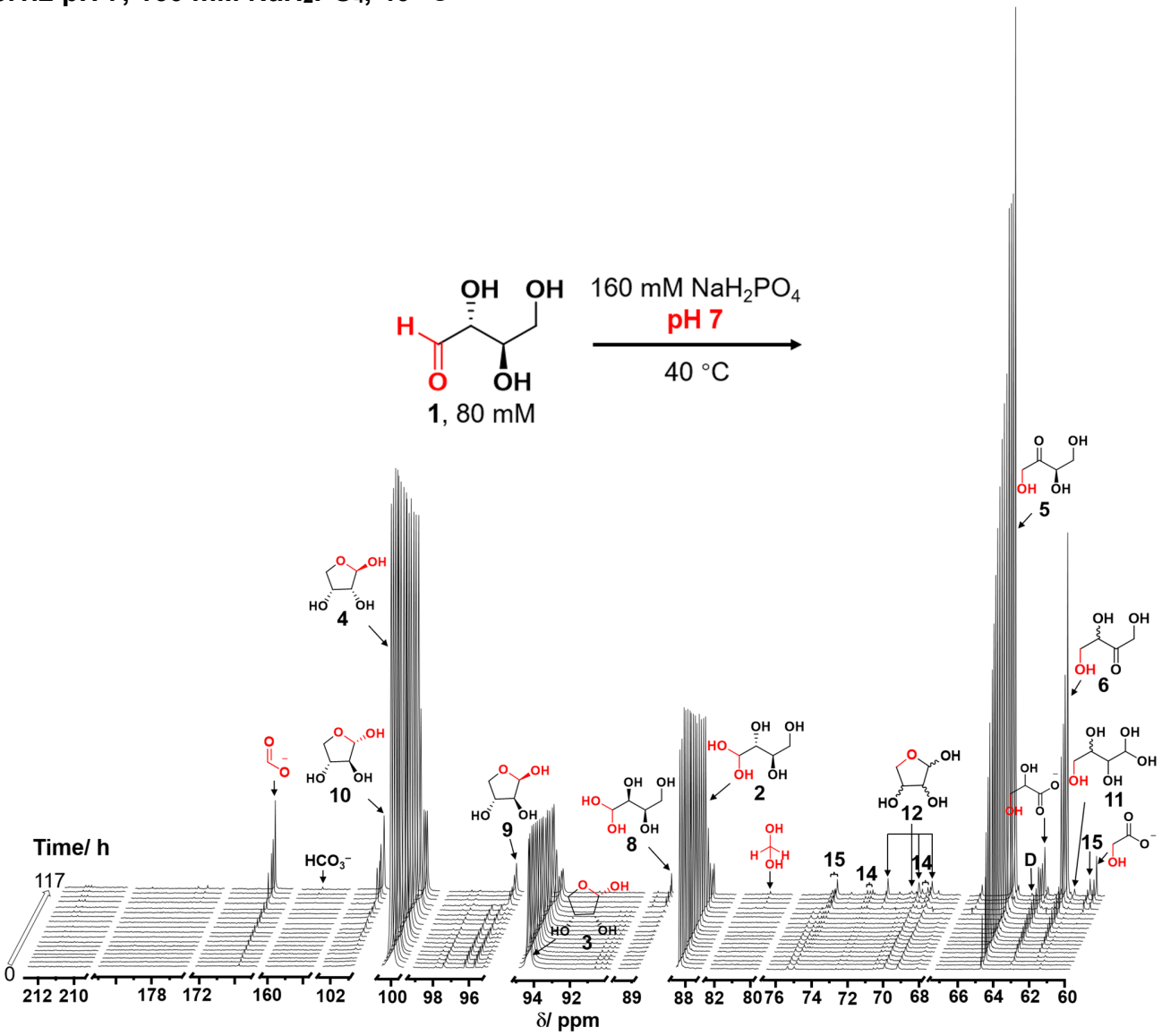

Figure S2. ^{13}C NMR spectra of 80 mM D-[1-^{13}C]-erythrose in 160 mM NaH_2PO_4 buffer at pH 7 at 40 °C over time. D-Erythrose (hydrate **2** and cyclic ring **3**, **4**), D-erythrulose **5**, *rac*-erythrulose **6**, D-threose (hydrate **8** and cyclic ring **9**, **10**), *rac*-tetrose (hydrate **11** and cyclic ring **12**) and diastereomeric C8 species (**14** and **15**) were observed in these spectra over time, and the peak intensities detected in each spectrum are recorded in **Table S3**. **D**: dihydroxyacetone. The rates of formation and disappearance of each species over a period of 117 hours is graphically displayed in **Figure S20**.

3.1.3 pH 8.5, 160 mM $NaHCO_3$, 40 °C

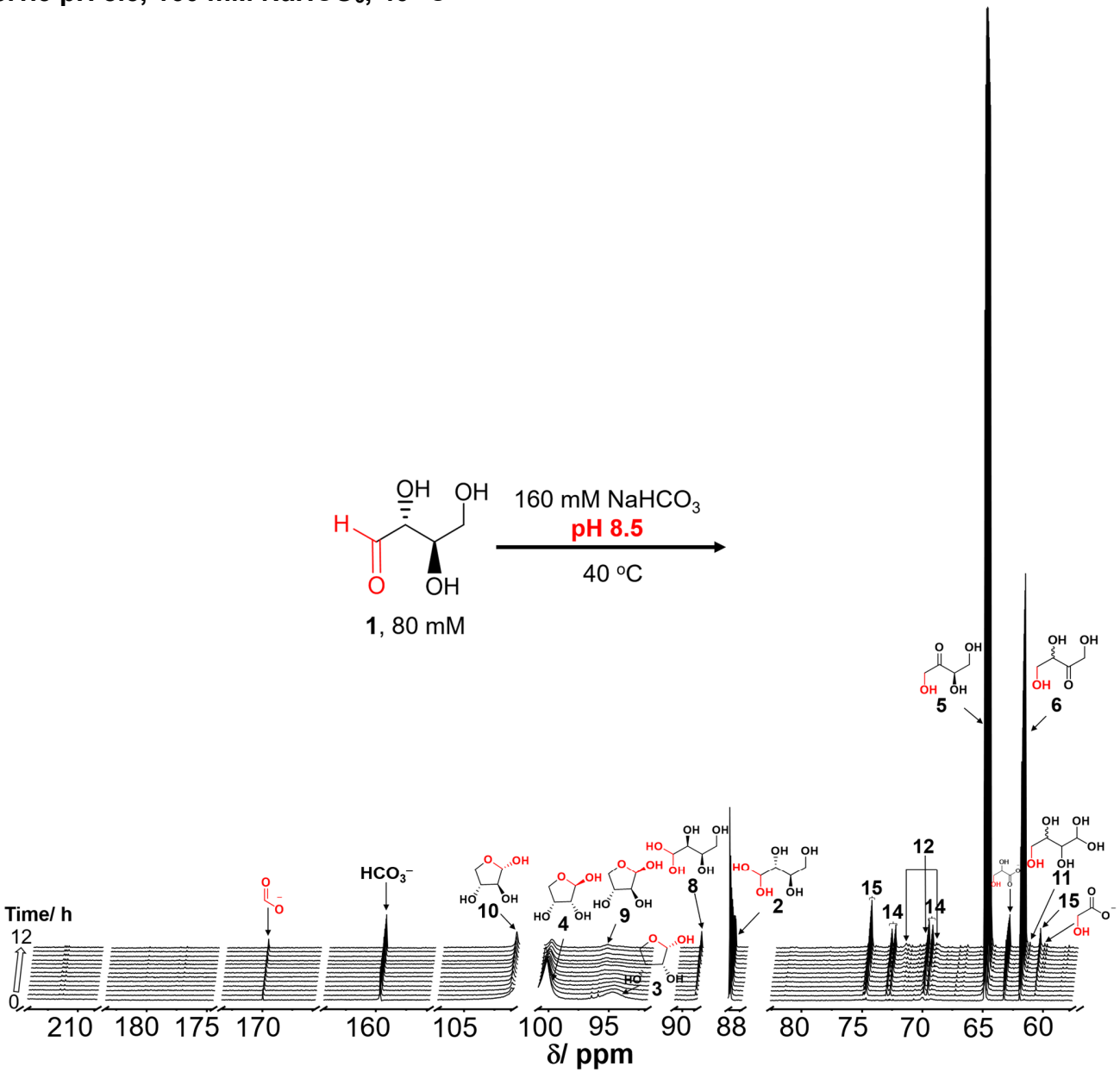

Figure S3. ^{13}C NMR spectra of 80 mM D-[1-^{13}C]-erythrose with 160 mM $NaHCO_3$ buffer at pH 8.5 at 40 °C over time. D-Erythrose (hydrate **2** and cyclic ring **3**, **4**), D-erythrulose **5**, *rac*-erythrulose **6**, D-threose (hydrate **8** and cyclic ring **9**, **10**), *rac*-tetrose (hydrate **11** and cyclic ring **12**) and diastereomeric C8 species (**14** and **15**) were observed in these spectra over time and the peak intensities detected in each spectrum are recorded in **Table S4**. The rates of formation and disappearance of each species over a period of 12 hours is graphically displayed in **Figure S21**.

3.1.4 pH 10, 160 mM $NaHCO_3$, 40 °C

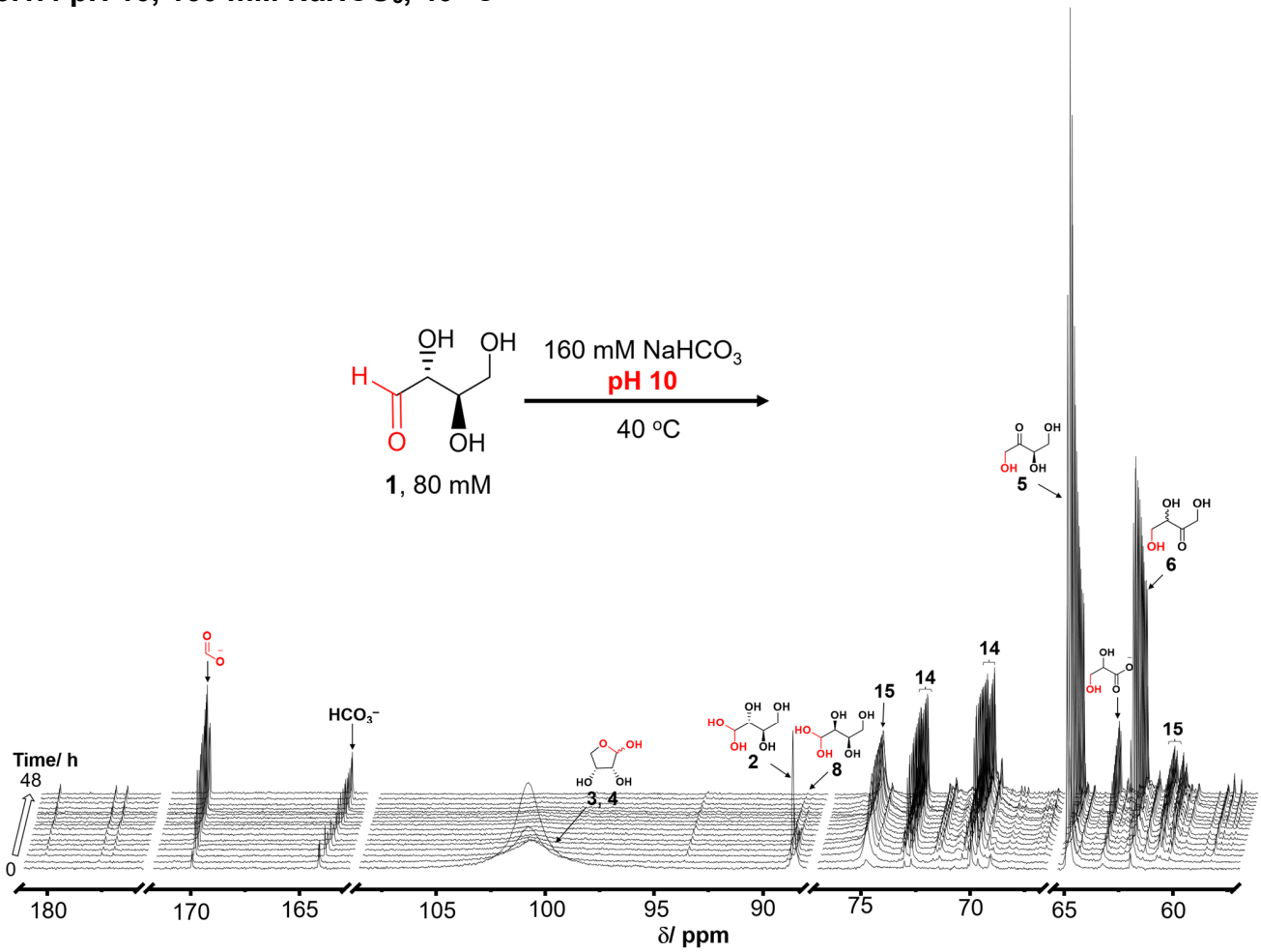

Figure S4. ^{13}C NMR spectra of 80 mM D-[1-^{13}C]-erythrose in 160 mM $NaHCO_3$ buffer at pH 10 at 40 °C over time. D-Erythrose (hydrate **2** and cyclic ring **3**, **4**), D-threose (hydrate **8**), D-erythrulose **5**, *rac*-erythrulose **6**, and diastereomeric C8 species (**14** and **15**) were observed in these spectra over time and the peak intensities detected in each spectrum are recorded in **Table S5**. Note that the signals of cyclic ring around 101 ppm are broad and difficult to determine separately. Therefore, this area around 101 ppm is assigned to be **3** and **4**. The rates of formation and disappearance of each species over a period of 48 hours is graphically displayed in **Figure S22**.

3.1.5 pH 7, 480 mM NaH_2PO_4, 40 °C

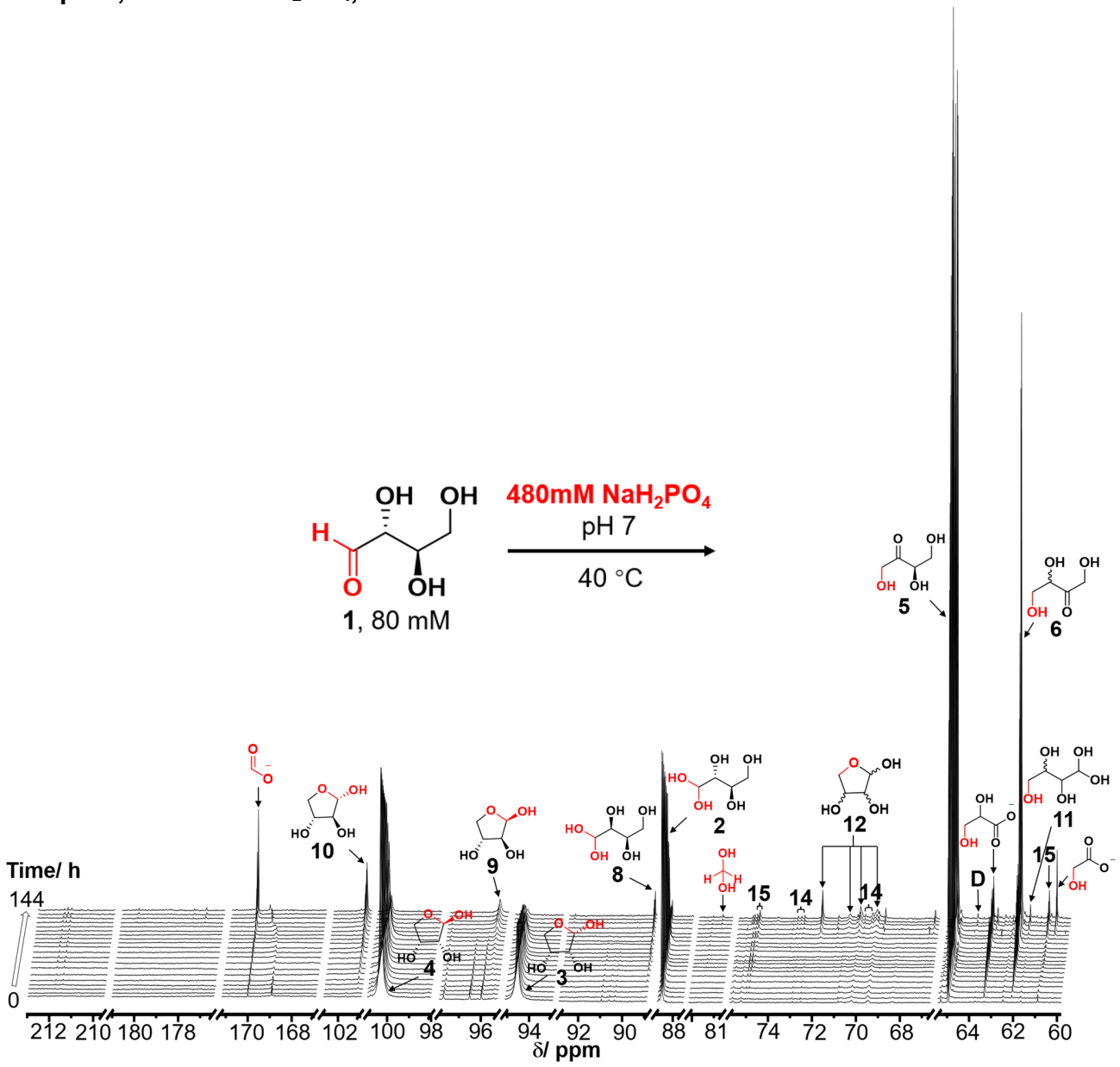

Figure S5. ^{13}C NMR spectra of 80 mM D-[1-^{13}C]-erythrose in 480 mM NaH_2PO_4 buffer at pH 7 at 40 °C over time. D-Erythrose (hydrate **2** and cyclic ring **3**, **4**), D-erythrulose **5**, *rac*-erythrulose **6**, D-threose (hydrate **8** and cyclic ring **9**, **10**), *rac*-tetrose (hydrate **11** and cyclic ring **12**), and diastereomeric C8 species (**14** and **15**) were observed in these spectra over time and the peak intensities detected in each spectrum are recorded in **Table S6**. The rates of formation and disappearance of each species over a period of 144 hours is graphically displayed in **Figure S23**.

3.1.6 pH 7, 160 mM cacodylate, 40 °C

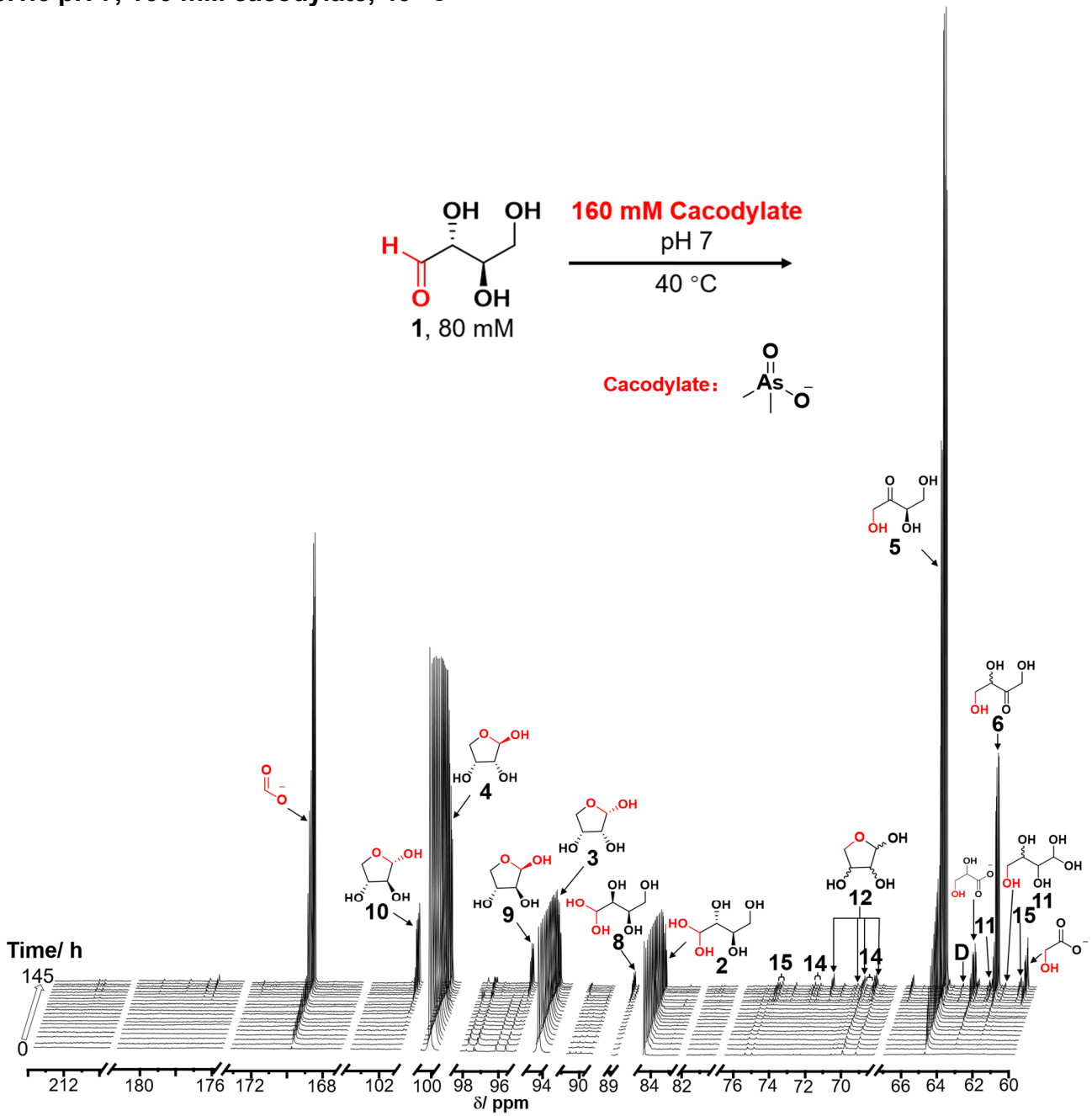

Figure S6. ^{13}C NMR spectra of 80 mM D-[1-^{13}C]-erythrose in 160 mM cacodylate buffer at pH 7 at 40 °C over time. D-Erythrose (hydrate **2** and cyclic ring **3**, **4**), D-erythrulose **5**, *rac*-erythrulose **6**, D-threose (hydrate **8**, cyclic ring **9**, **10**), *rac*-tetrose (hydrate **11** and cyclic ring **12**) and diastereomeric C8 species (**14** and **15**) were observed in these spectra over time and the peak intensities detected in each spectrum are recorded in **Table S7**. The rates of formation and disappearance of each species over a period of 145 hours is graphically displayed in **Figure S24**.

3.2 D-[4-^{13}C]-Erythrose

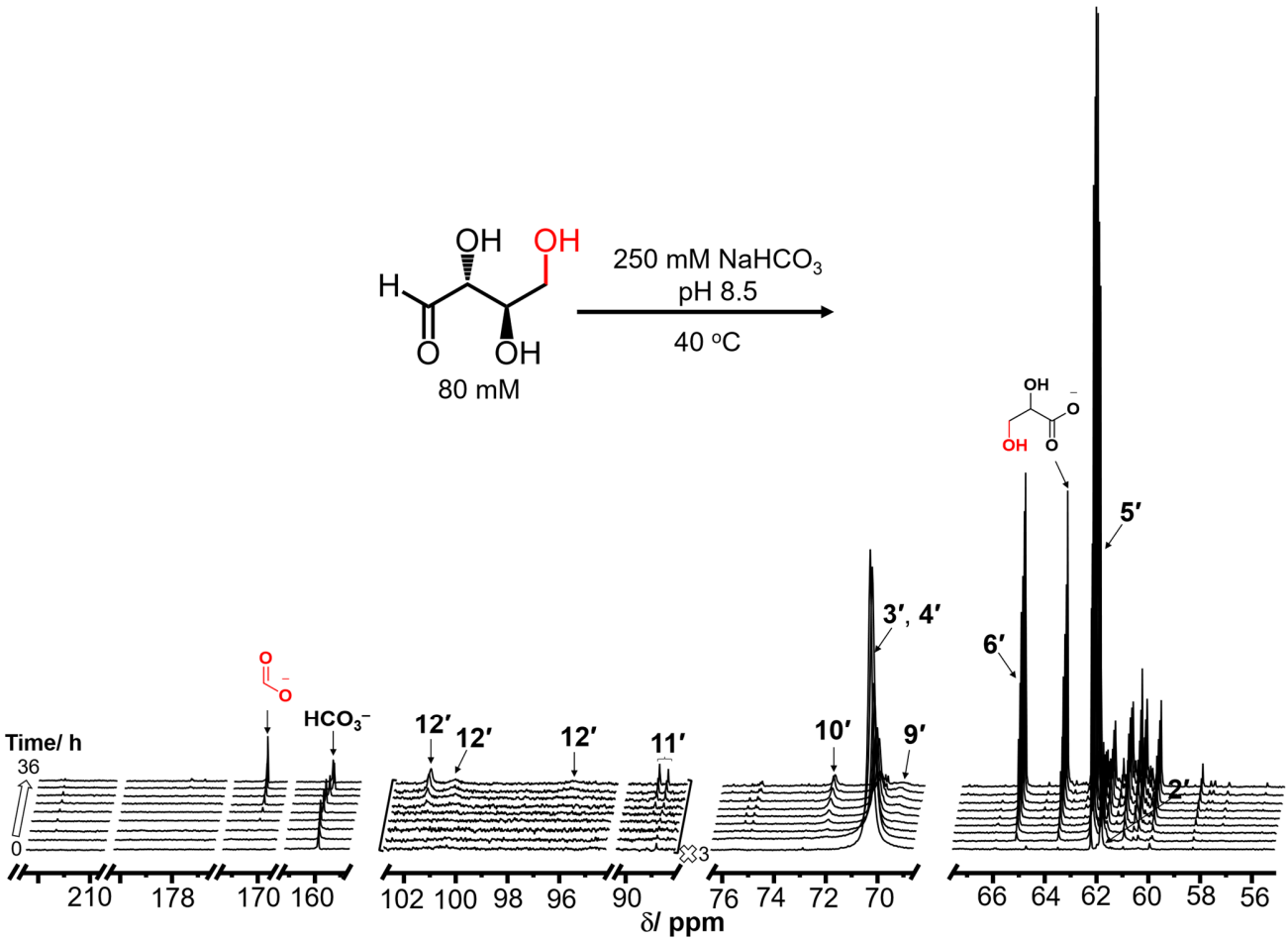

Figure S7. ^{13}C NMR spectra of 80 mM D-[4-^{13}C]-erythrose in 250 mM $NaHCO_3$ buffer at pH 8.5 at 40 °C over time. D-Erythrose (hydrate **2'** and cyclic ring **3', 10'**), D-erythrulose **5'**, *rac*-erythrulose **6'**, D-threose (cyclic ring **9'** and **10'**), *rac*-tetrose (hydrate **11'** and cyclic ring **12'**) were observed in these spectra over time and the peak intensities detected in each spectrum are recorded in **Table S8**. **D**: dihydroxyacetone. The rates of formation and disappearance of each species over a period of 36 hours is graphically displayed in **Figure S25**.

3.3 D-[1-^{13}C]-Erythrose and D-[4-^{13}C]-Erythrose

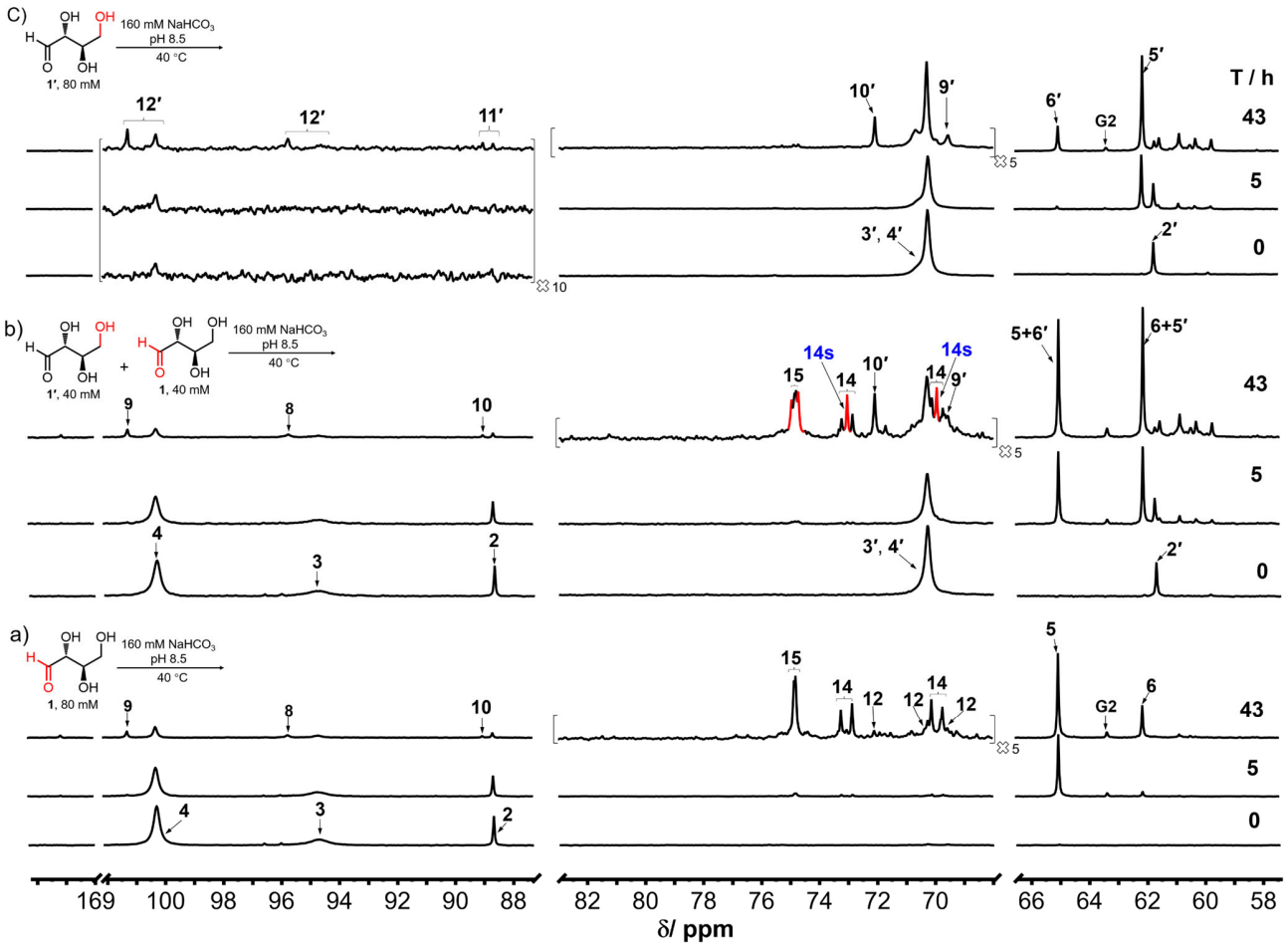

Figure S8. ^{13}C NMR spectra for carbonyl migration of a) 80 mM [1-^{13}C]-erythrose b) 40 mM [1-^{13}C]-erythrose and 40 mM [4-^{13}C]-erythrose c) 80 mM [4-^{13}C]-erythrose at 0, 5 and 43 hours at 40 °C, pH 8.5 in presence of 160 mM bicarbonate buffer. The result shows that 1-^{13}C erythrose tends to be consumed at a similar rate in both **Figure S8a** and **Figure S8b**. Moreover, in the spectra of **Figure S8b**, the total peak intensity of 1-^{13}C-D-erythrulose **5** and 4-^{13}C-*rac*-erythrulose **6′** at 65.0 ppm is almost equal to the total peak intensity of 1-^{13}C-*rac*-erythrulose **6** and 4-^{13}C-D-erythrulose **5′** at 62.0 ppm at 5 and 43 hours. This observation indicates that a similar distribution of D-erythrulose and *rac*-erythrulose was produced when the reaction was carried out in the mixture of 1-^{13}C-D-erythrose and 4-^{13}C-D-erythrose, as when it was carried out with 1-^{13}C-D-erythrose or 4-^{13}C-D-erythrose, separately. It should be note that, similar products were observed in **Figure S8b**, as compared to those in **Figure S8a** and **FigureS8c**, except for four new peaks marked in red. These peaks are assigned to octuloses. For example, as shown in **Figure S8a**, 1-^{13}C-D-erythrose and 1-^{13}C-D-erythrulose were abundant after 5 h when the reaction was carried out using 1-^{13}C-erythrose, and the aldol reaction of 1-^{13}C-D-erythrose and 1-^{13}C-D-erythrulose leads to the formation of octuloses 14 (two doublets in the 69.5–70.0 and 72.5–73.5 ppm region). Meanwhile, 1-^{13}C-D-erythrose, 1-^{13}C-D-erythrulose, 4-^{13}C-D-erythrose, 4-^{13}C-D-erythrulose were enriched at the initial 5 h when both 1-^{13}C-D-erythrose and 4-D-^{13}C erythrose are mixed in **Figure S8b**. In addition to the formation of octuloses **14**, this fact also resulted in the formation of octuloses **14s** (singlets in the 69.8 and 72.9 ppm). The samples from each reaction after 43 hours were also measured by mass spectroscopy and shown in **Figure S18**.

3.4 D-[1-^{13}C]-Threose

3.4.1 pH 8.5, 160 mM $NaHCO_3$, 40 °C

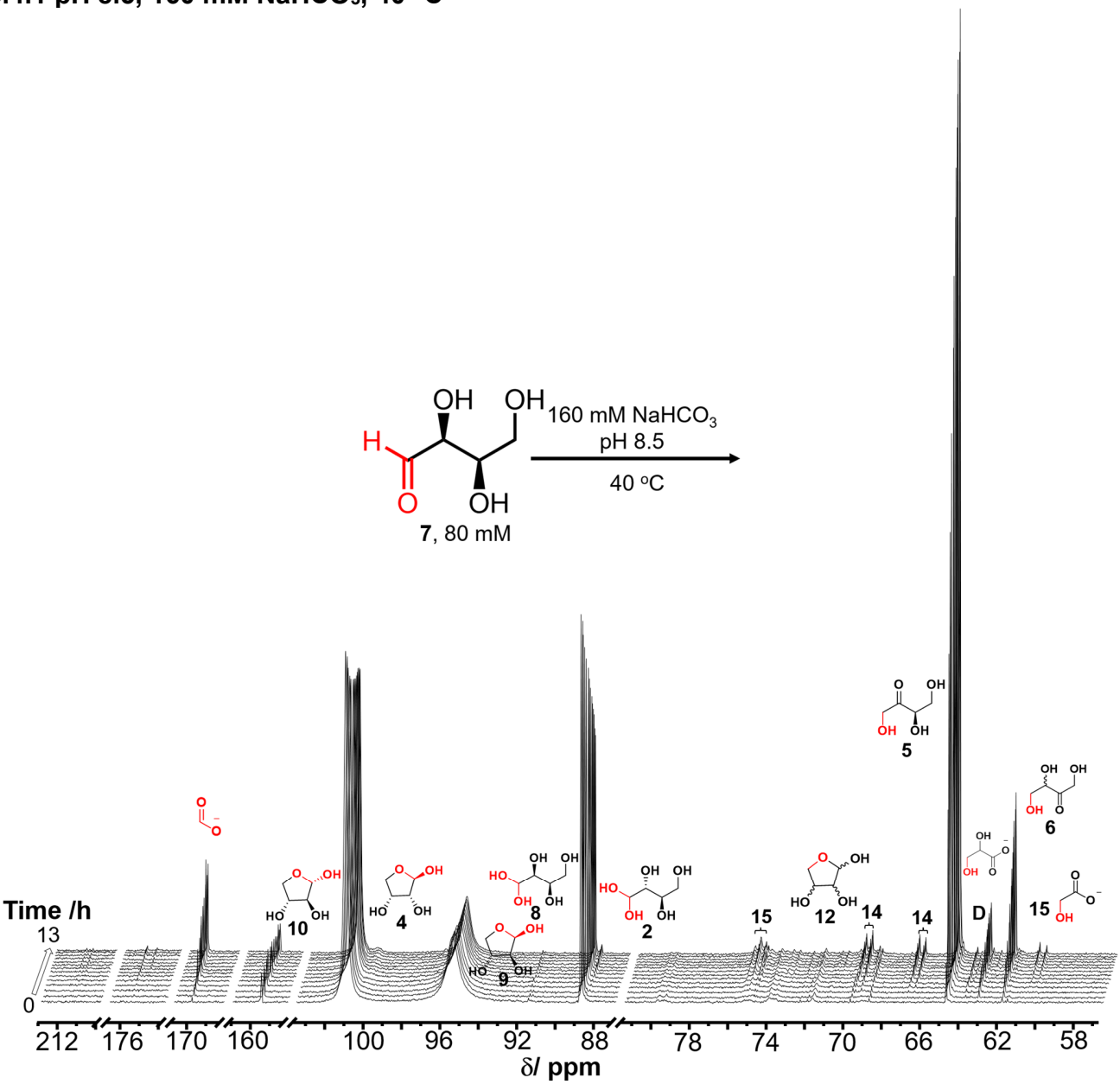

Figure S9. ^{13}C NMR spectra of 80 mM D-[1-^{13}C]-threose in 160 mM $NaHCO_3$ buffer at pH 8.5 at 40 °C over time. D-Threose (hydrate **8** and cyclic ring **9, 10**), D-erythrulose **5**, *rac*-erythrulose **6**, D-erythrose (hydrate **2** and cyclic ring **4**), *rac*-tetrose (cyclic ring **12**) and diastereomeric C8 species (**14** and **15**) were observed in these spectra over time and the peak intensities detected in each spectrum are recorded in **Table S9**. **D**: dihydroxyacetone.

3.4.2 pH 8.5, 160 mM $NaHCO_3$, 40 °C, degassed by N_2 gas

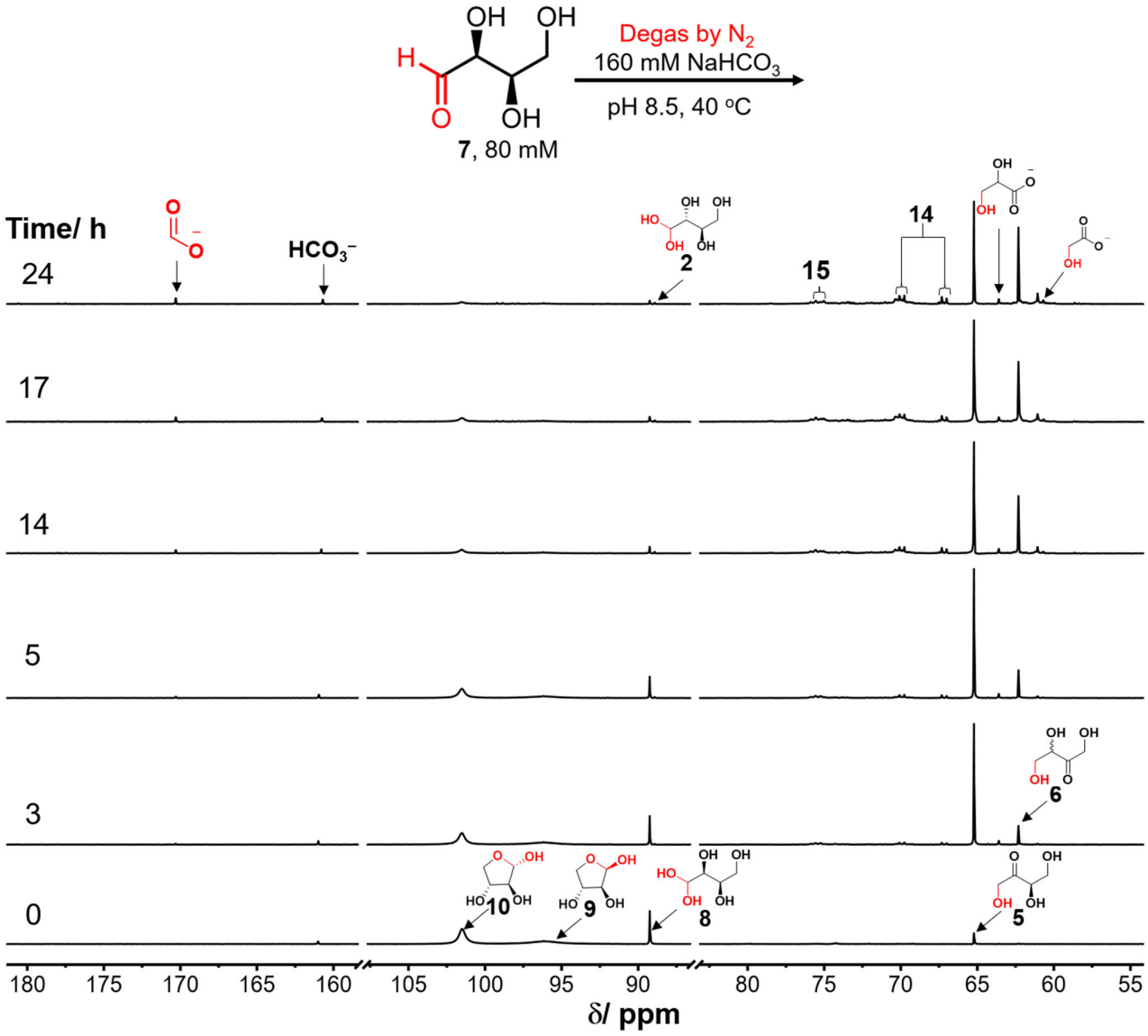

Figure S10. ^{13}C NMR spectra of 80 mM D-[1-13C]-threose in 160 mM $NaHCO_3$ buffer with a N_2 degassing process at pH 8.5 at 40 °C over time. 364 μL of 110 mM D-[1-13C]-threose stock solution was mixed with 56 μL of H2O, and then degassed by N_2 gas for 20 mins. The stock $NaHCO_3$ solution was also degassed by N_2 gas for 20 mins before mixing with the threose solution. The mixed solution was transferred into the NMR tube and degassed by N_2 gas for 2 mins, and pH increased from 8.5 to 9 after degassing. The rate of formation of formate over a period of 24 hours is graphically displayed in **Figure S26a**.

3.4.3 pH 8.5, 160 mM $NaHCO_3$, 40 °C, enriched with air

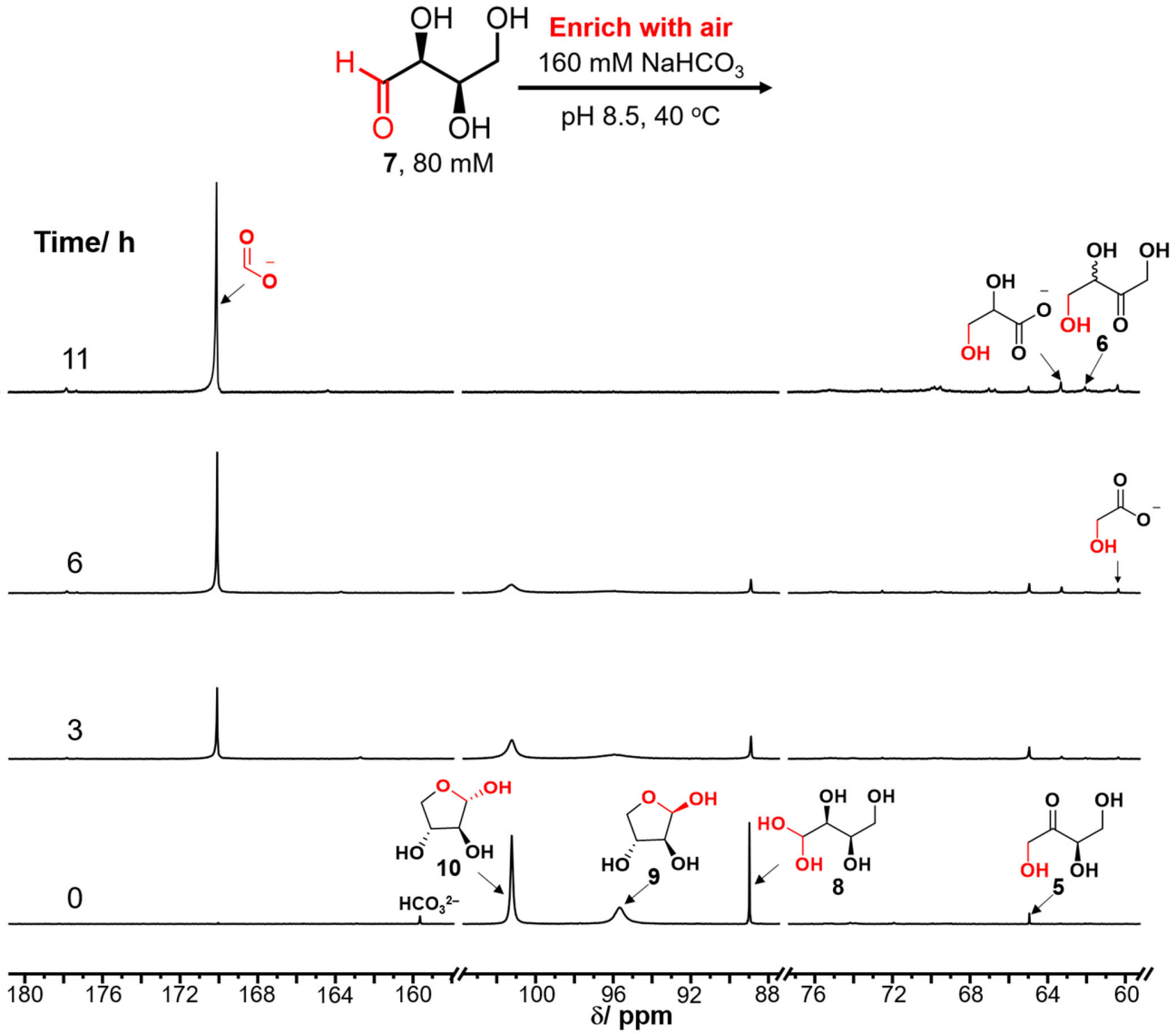

Figure S11. ^{13}C NMR spectra of 80 mM D-[1-^{13}C]-threose in 160 mM $NaHCO_3$ buffer with air-enrich process at pH 8.5 at 40 °C over time. 364 μL of 110 mM D-[1-^{13}C]-threose stock solution was mixed with 56 μL of H_2O and 80 μL of 1 M $NaHCO_3$ stock solution at pH 8.5 in a 1.5 mL Eppendorf tube to produce a 0.5 mL aqueous solution containing 80 mM D-[1-^{13}C]-threose and 160 mM $NaHCO_3$. This solution was loaded into an NMR tube and kept slowly bubbling with air during heating at 40 °C. The pH increased from 8.5 to 10 during the bubbling. The rates of formation and disappearance of each species over a period of 11 hours is graphically displayed in **Figure S26b**.

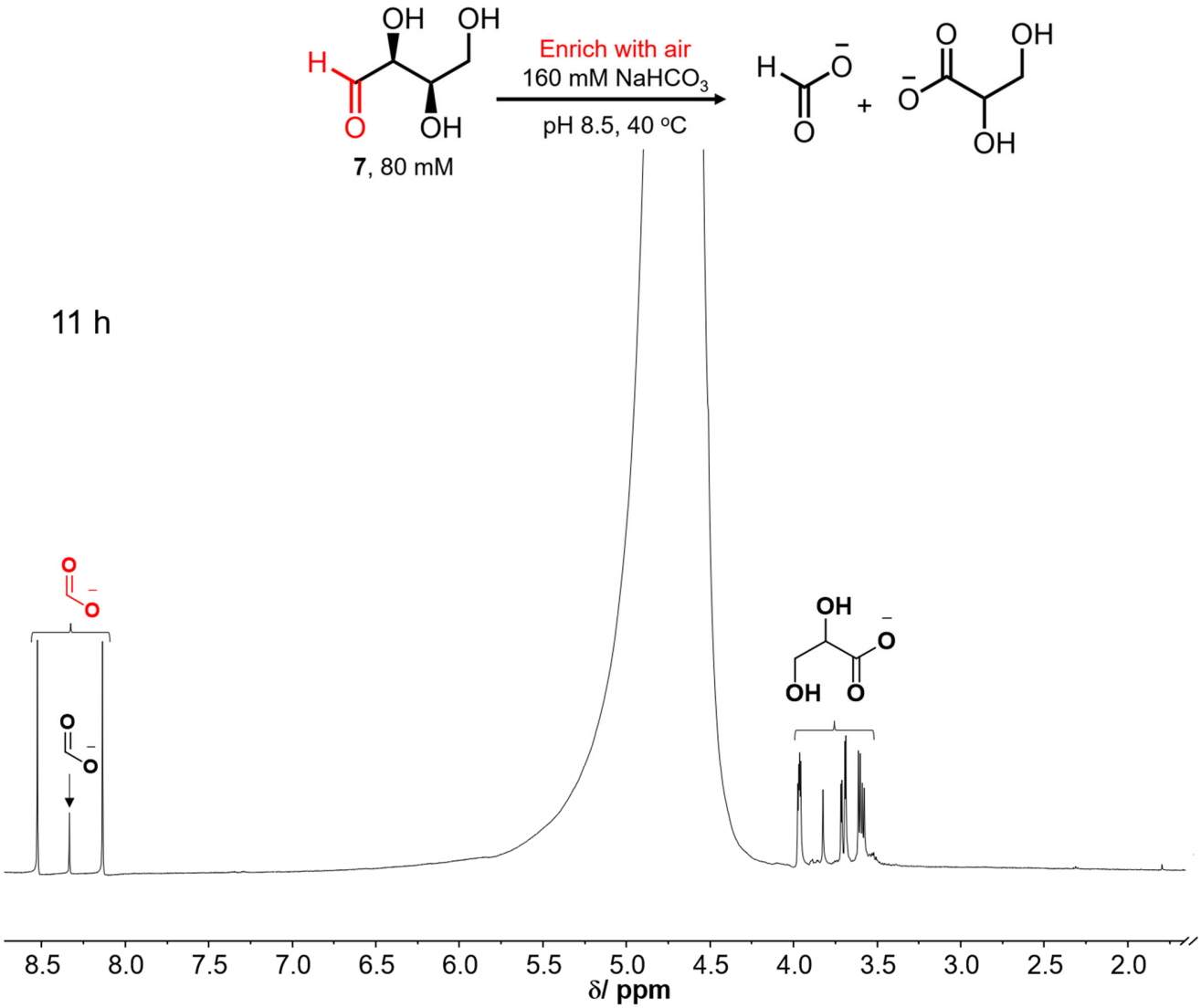

Figure S12. ^{1}H NMR spectrum of 80 mM D-[1-^{13}C]-threose in 160 mM $NaHCO_3$ buffer with air-enrich process at pH 8.5 at 40 °C. Formate and glycerate were identified as major product. This result suggests that the oxidation of D-[1-^{13}C]-threose generates formate and glycerate. Both non-^{13}C labelled formate and ^{13}C labelled formate were detected in this spectrum. Note that the ^{13}C labelled formate was determined by the obtained $J_{1H,\ 13C}$= 194.8 Hz.

3.5 ^{13}C-Formaldehyde

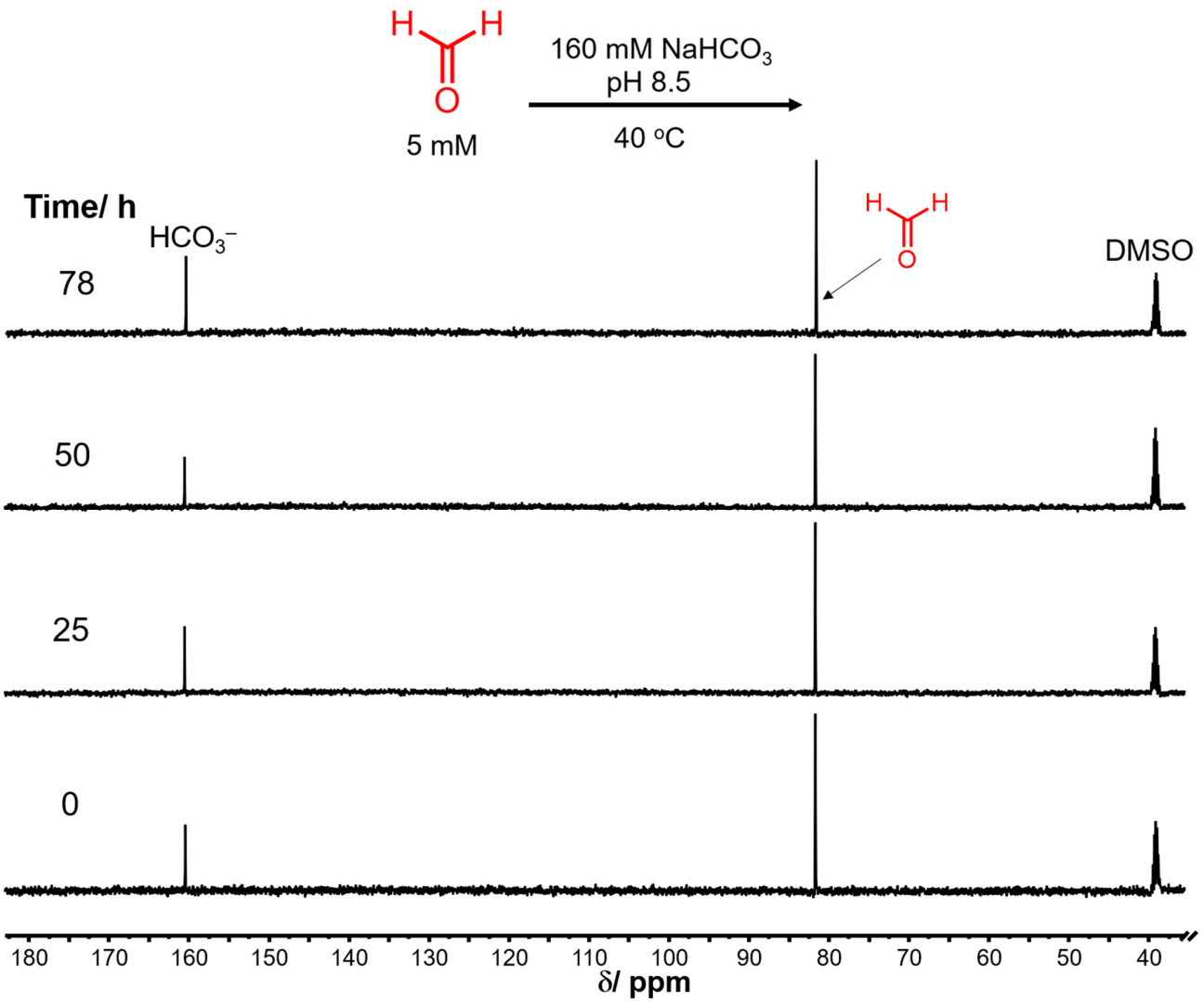

Figure S13. ^{13}C NMR spectra of 5 mM ^{13}C-formaldehyde in 160 mM $NaHCO_3$ at pH 8.5 at 40 °C. 0.31 μL of 20% ^{13}C-formaldehdye stock solution (8 M) was mixed with 80 μL of 1 M $NaHCO_3$ and 420 μL of H_2O to produce a 0.5 mL aqueous solution containing 5 mM ^{13}C-formaldehdye and 160 mM $NaHCO_3$ buffered. This solution was loaded into an NMR tube and heated to 40 °C. No formate was observed over time, which suggests that the formation of formate is not proceeding through formaldehyde pathway.

3.6 Glycolaldehyde

3.6.1 pH 8.5, 500 mM $NaHCO_3$, 25 °C

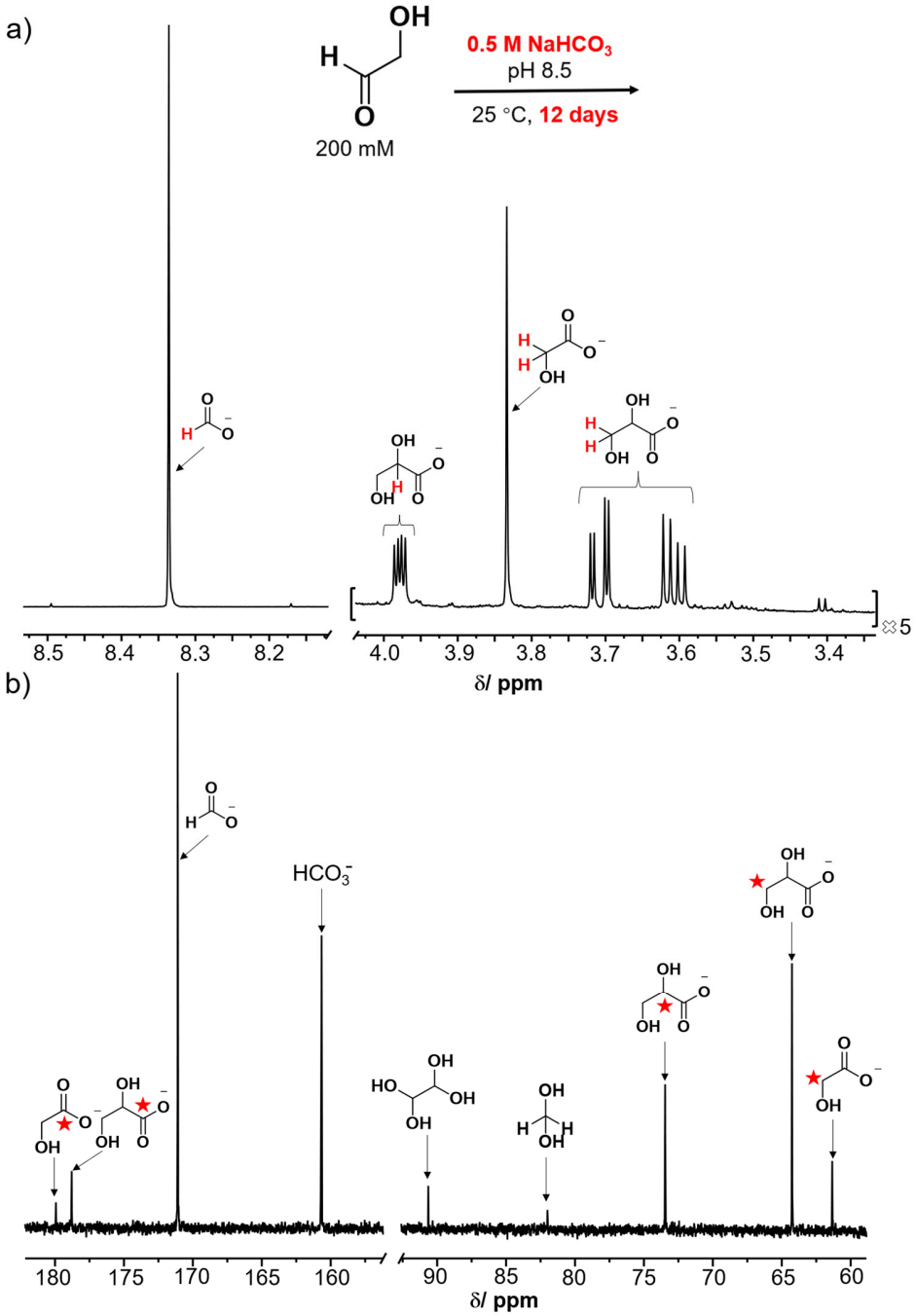

Figure S14. a) ^{1}H-NMR spectrum of the reaction mixture of 0.2 M glycolaldehyde in 0.5 M bicarbonate buffer after 12 days and formation of glycerate, glycolate and formate as products. b) ^{13}C-NMR spectrum of the reaction mixture of 0.2 M glycolaldehyde in 0.5 M bicarbonate buffer after 12 days and formation of glycerate, glycolate and formate as major products. Glyoxal and formaldehyde were also observed.

3.6.2 pH 8.5, 1 M $NaHCO_3$, 25 °C

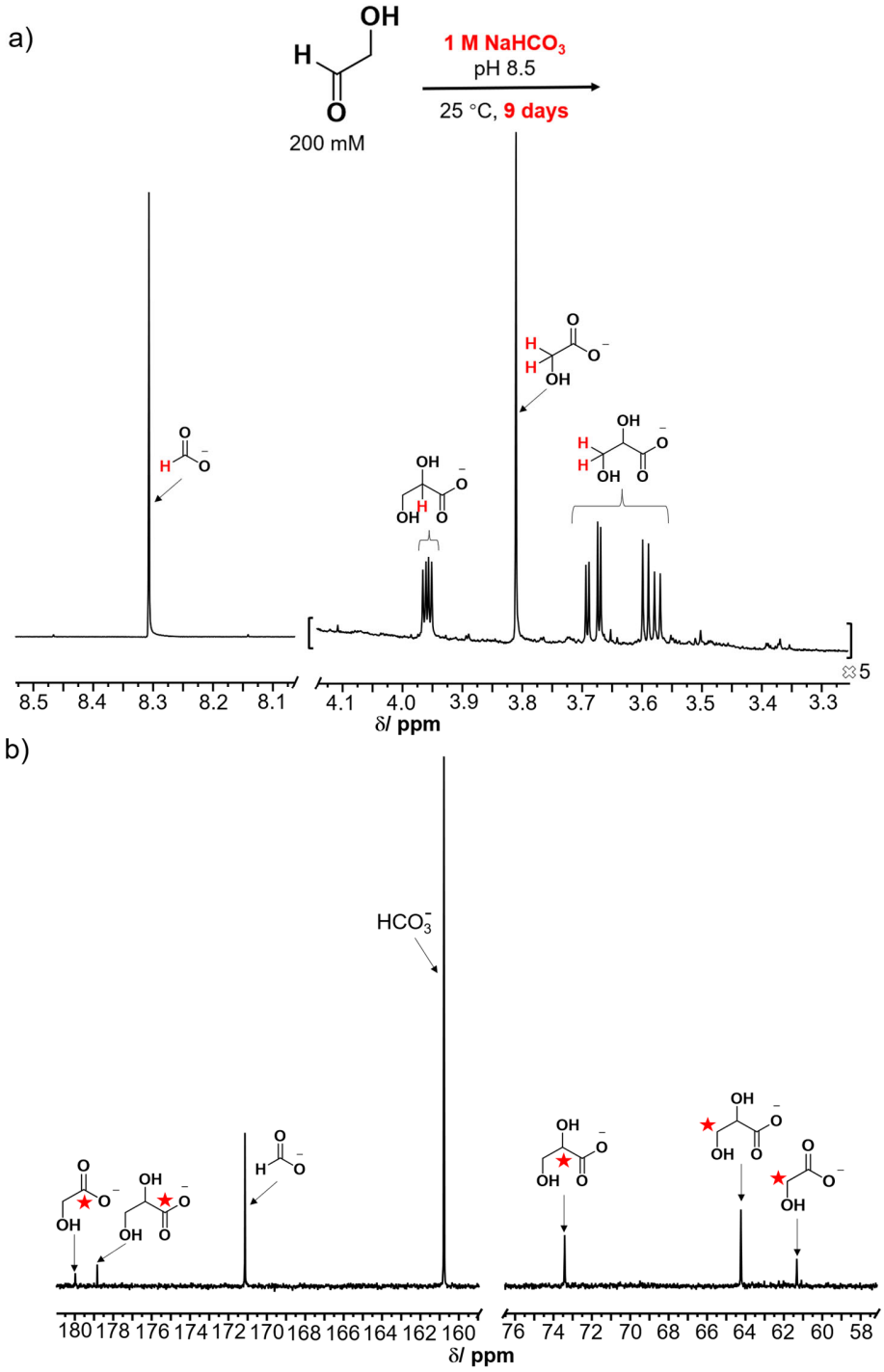

Figure S15. a) ^{1}H-NMR spectrum of the reaction mixture of 0.2 M glycolaldehyde in 1 M bicarbonate buffer after 9 days and formation of glycerate, glycolate and formate as products. b) ^{13}C-NMR spectrum of the reaction mixture of 0.2 M glycolaldehyde in 1 M bicarbonate buffer after 9 days and formation of glycerate, glycolate and formate as major products.

3.6.3 pH 8.5, 500 mM $NaHCO_3$, 25 °C, degas by N_2

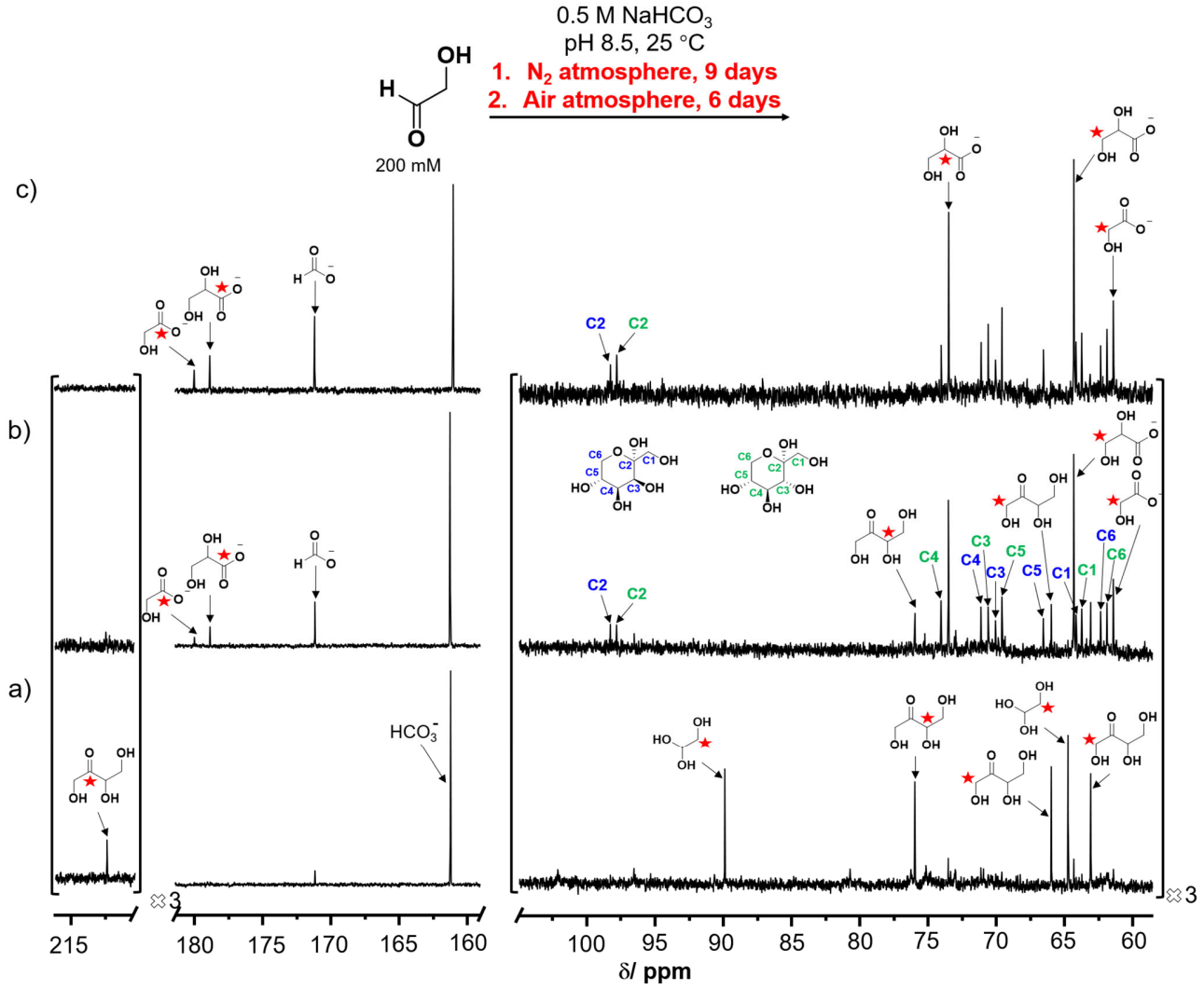

Figure S16. ^{13}C-NMR spectra of the reaction mixture of 0.2 M glycolaldehyde in 0.5 M bicarbonate buffer. a) under N_2 for 2 days. Erythrulose was observed to be the major product, which arose from carbonyl migration of newly formed tetroses from aldol reaction of glycolaldehyde. b) under N_2 for 9 days, C6 sugars involving sorbose and tagatose, together with glycolate, glycerate and formate were found as the main products, while the signal intensity of glycolaldehyde and erythrulose decreased. c) under air for 6 days following, more glycolate, glycerate and formate were observed.

3.6.4 pH 7, 500 mM NaH_2PO_4, 40 °C

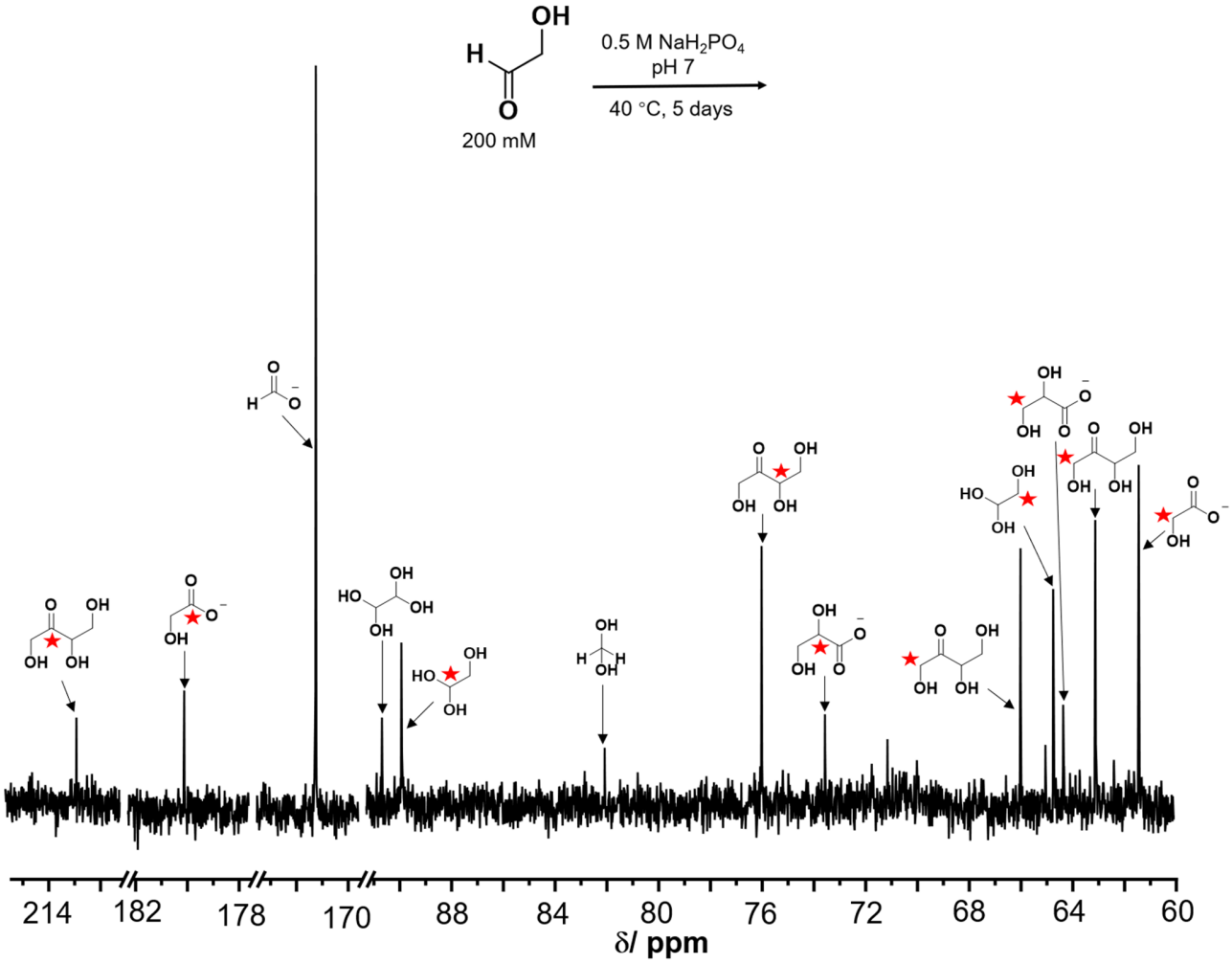

Figure S17. ^{13}C-NMR spectra of the reaction mixture of 0.2 M glycolaldehyde in 0.5 M phosphate buffer at 40°C for 5 days showing glycerate, glycolate, glyoxal hydrate and formate as main products from the oxidation of glycolaldehyde and tetrose/ tetrulose.

4. Mass spectra

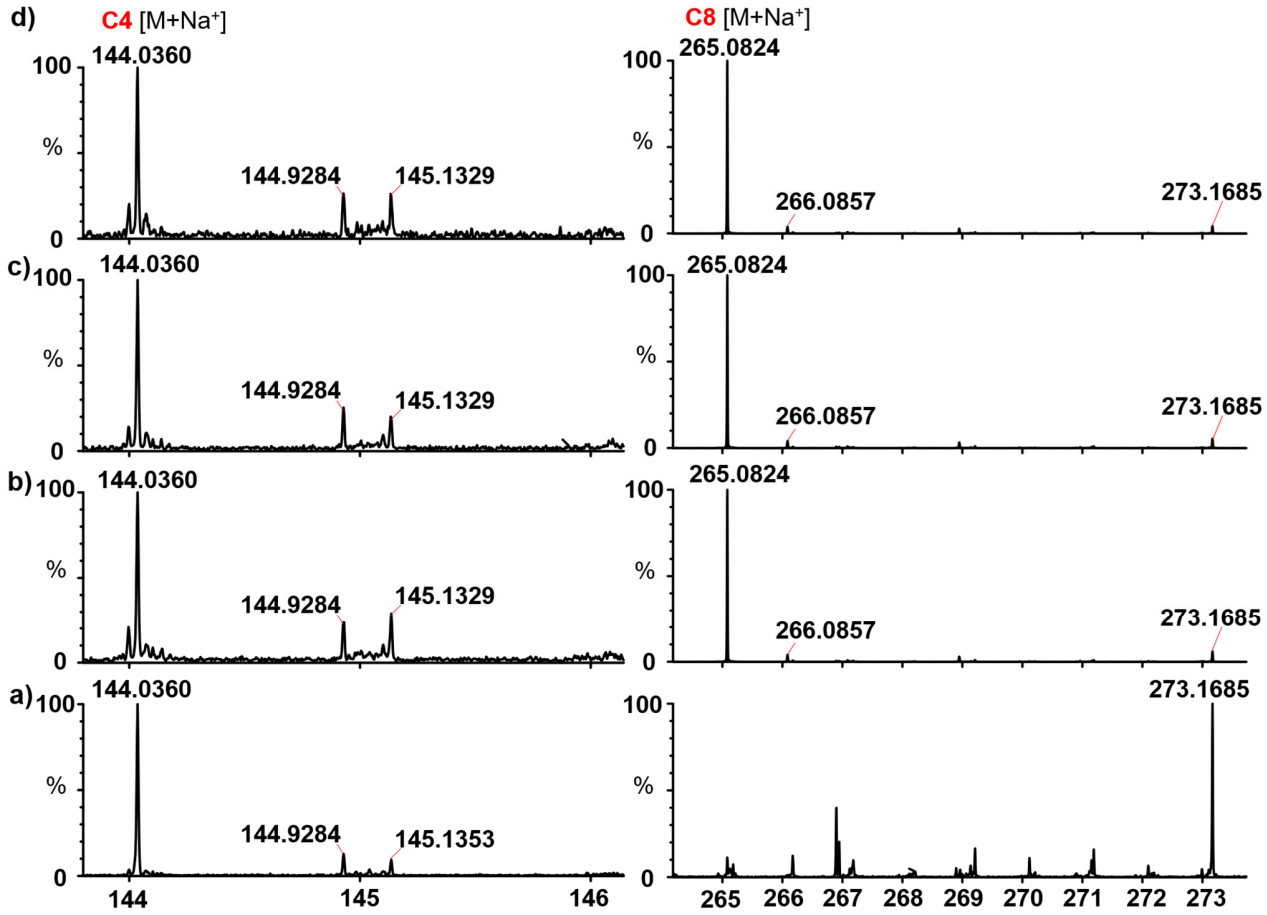

Figure S18. MS spectra for a) [1-^{13}C]-erythrose at 0 hour b) [1-^{13}C]-erythrose after 43 hours c) [4-^{13}C]-erythrose after 43 hours d) [1-^{13}C]-erythrose and [4-^{13}C]-erythrose after 43 hours. The MS signals of 144.0360 and 265.0824 were assigned to tetroses (with one labelled ^{13}C) and octuloses (with two labelled ^{13}C). The result shows that MS signals of tetroses (with one labelled ^{13}C) and octuloses (with two labelled ^{13}C) have no significant difference between each reaction in 1-^{13}C erythrose, 4-^{13}C-erythrose and the mixture of 1-^{13}C erythrose and 4-^{13}C-erythrose after 43 hours. If erythrose itself would undergo retro-aldol under these reaction conditions, then the aldol reactions of resulting glycolaldehyde could lead to other recombination products, thus affecting the product distribution and interfere with the carbonyl-migration analysis. However, no doubly ^{13}C-labeled erythrose (or erythrulose) was detected in the mixed reaction of D-[1-^{13}C]-erythrose and D-[4-^{13}C]-erythrose, an observation suggesting that a retro-aldol of the individual erythrose were not occurring at the detectable limits of these analytical techniques. The only doubly ^{13}C-labeled products observed were peaks corresponding to octuloses consistent with aldol reaction between erythrose/erythrulose combinations.

5. Additional figures

5.1 D-[1-^{13}C]-Erythrose

5.1.1 pH 5, 160 mM NaOAc, 40 °C

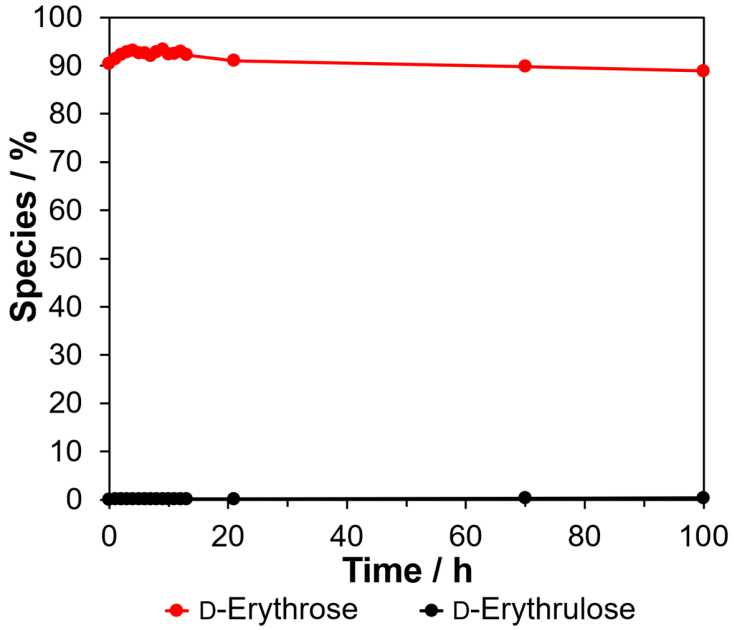

Figure S19. D-Erythrose carbonyl migration: the rates of disappearance of D-erythrose and the formation of D-erythrulose at a pH of 5 in 160 mM NaOAc buffer at 40 °C over a period of 100 hours.

5.1.2 pH 7, 160 mM NaH_2PO_4, 40 °C

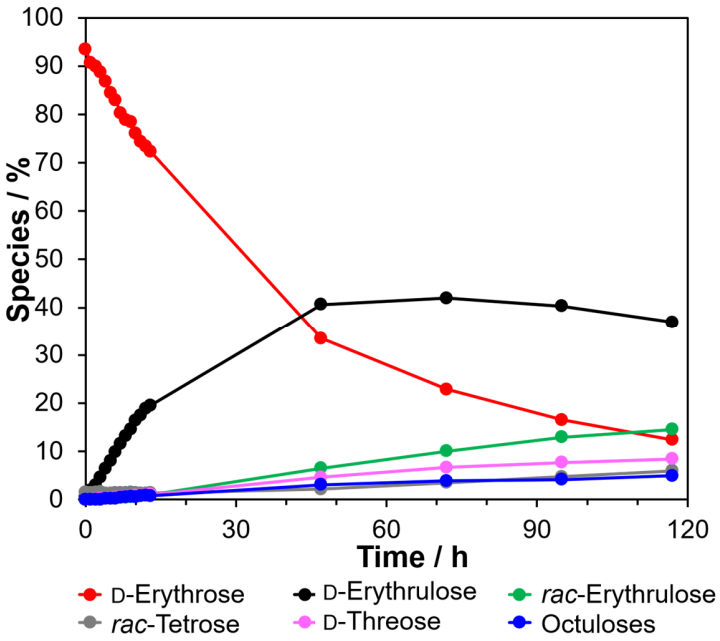

Figure S20. D-Erythrose carbonyl migration: the rates of disappearance of D-erythrose and the formation of D-erythrulose, *rac*-erythrulose, *rac*-tetrose, D-threose and diastereomeric octuloses at a pH of 7 in 160 mM NaH_2PO_4 buffer at 40 °C over a period of 117 hours.

5.1.3 pH 8.5, 160 mM $NaHCO_3$, 40 °C

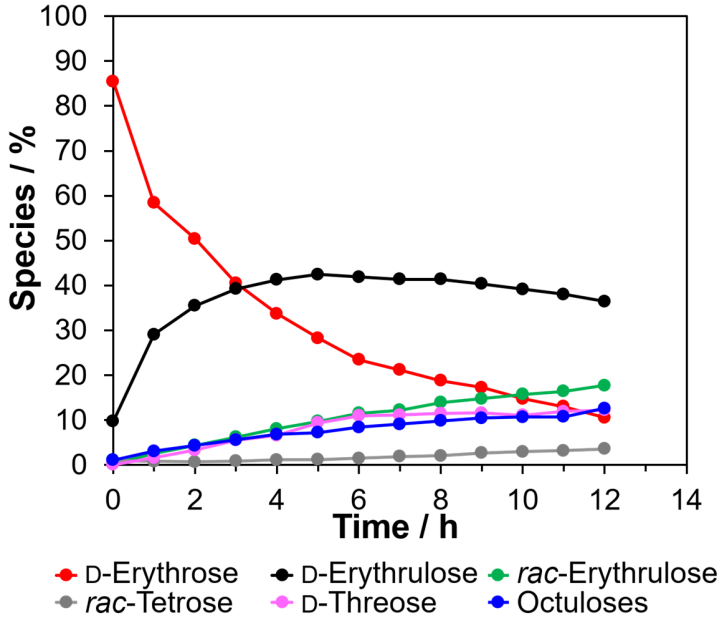

Figure S21. D-Erythrose carbonyl migration: the rates of disappearance of D-erythrose and the formation of D-erythrulose, *rac*-erythrulose, *rac*-tetrose, D-threose and diastereomeric octuloses at a pH of 8.5 in 160 mM $NaHCO_3$ buffer at 40 °C over a period of 12 hours.

5.1.4 pH 10, 160 mM $NaHCO_3$, 40 °C

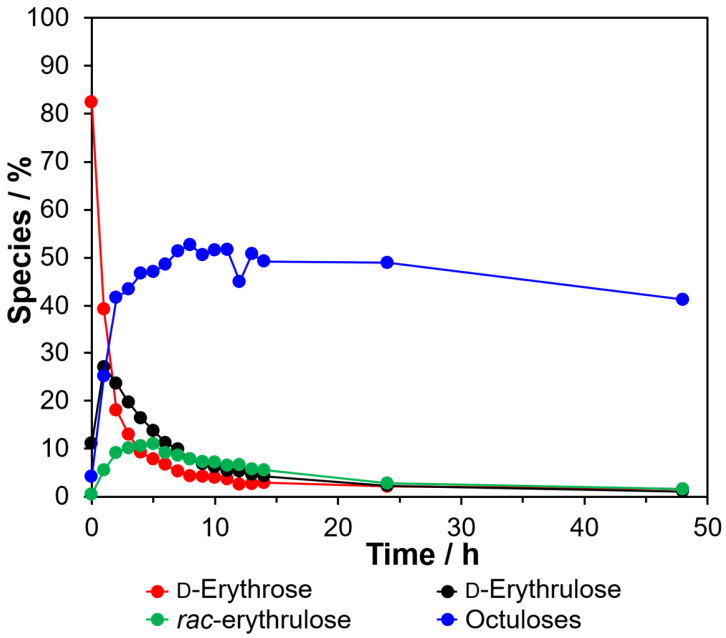

Figure S22. D-Erythrose carbonyl migration: the rates of disappearance of D-erythrose and the formation of D-erythrulose, *rac*-erythrulose and diastereomeric octuloses at a pH of 10 in 160 mM $NaHCO_3$ buffer at 40 °C over a period of 48 hours.

5.1.5 pH 7, 480 mM NaH_2PO_4, 40 °C

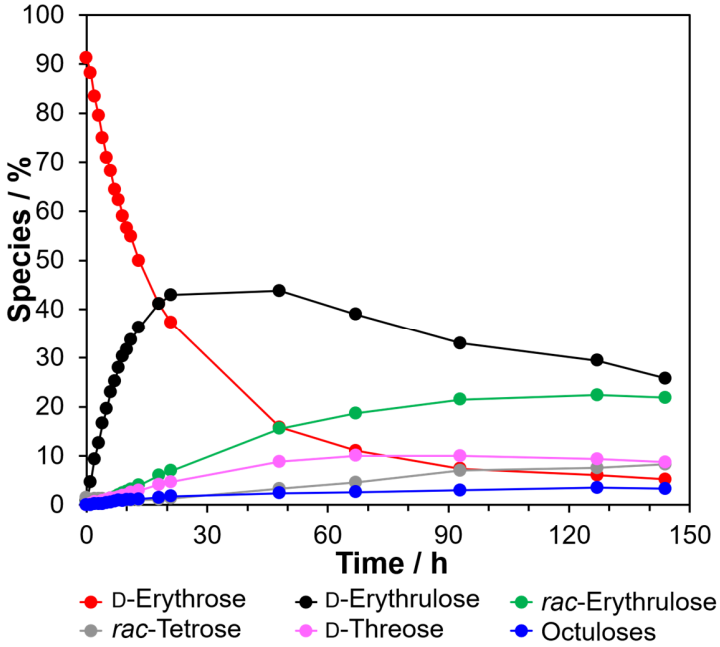

Figure S23. D-Erythrose carbonyl migration: the rates of disappearance of D-erythrose and the formation of D-erythrulose, *rac*-erythrulose, *rac*-tetrose, D-threose and diastereomeric octuloses at a pH of 7 in 480 mM NaH_2PO_4 at 40 °C over a period of 144 hours.

5.1.6 pH 7, 160 mM cacodylate, 40 °C

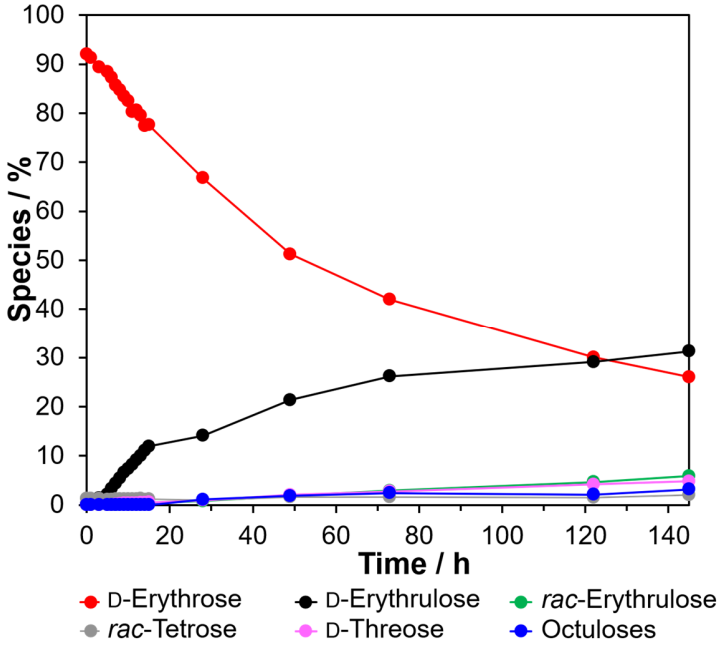

Figure S24. D-Erythrose carbonyl migration: the rates of disappearance of D-erythrose and the formation of D-erythrulose, *rac*-erythrulose, *rac*-tetrose, D-threose and diastereomeric octuloses at a pH of 7 in 160 mM sodium cacodylate at 40 °C over a period of 145 hours.

5.2 D-[4-^{13}C]-Erythrose, pH 8.5, 250 mM $NaHCO_3$, 40 °C

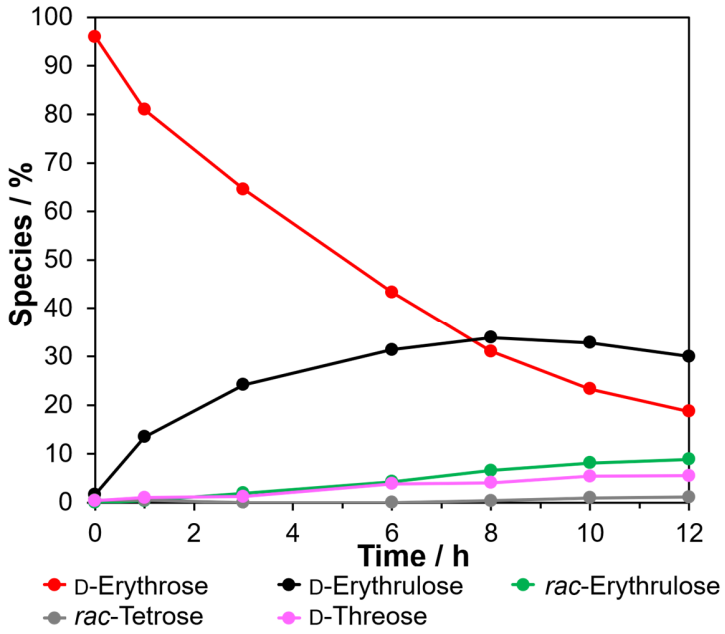

Figure S25. D-4-^{13}C-Erythrose carbonyl migration: the rates of disappearance of D-erythrose and the formation of D-erythrulose, *rac*-erythrulose, *rac*-tetrose, D-threose at pH 8.5 over a 12 hour-time period at 40 ^{o}C.

5.3 D-[1-^{13}C]-Threose, degas by N_2 or enrich with air

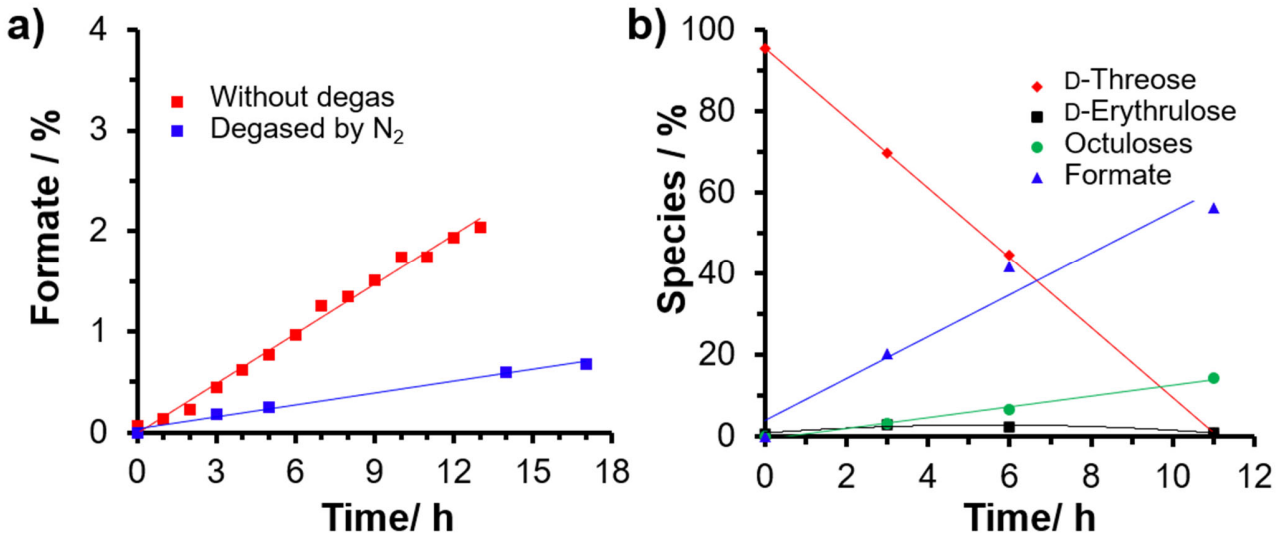

Figure S26. The rate of formation of formate arising from decomposition of threose at pH 8.5 at 40 °C. a) With and without a N_2 degassing process. b) Enrich with air.

5.4 Scheme S1 for formation of diastereomeric octuloses

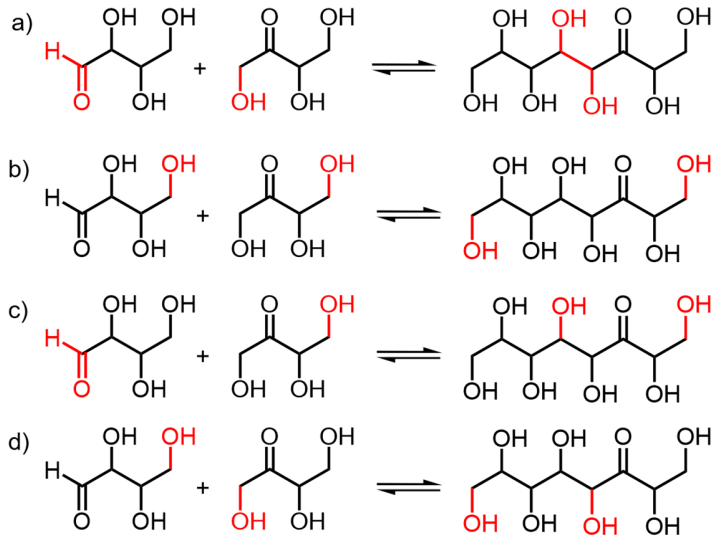

Scheme S1. Formation of diastereomeric octuloses via aldol reactions at 25 °C, pH 8.5.

5.5 Scheme S2 for enediol(ate) and 1,2-hydride shift pathway

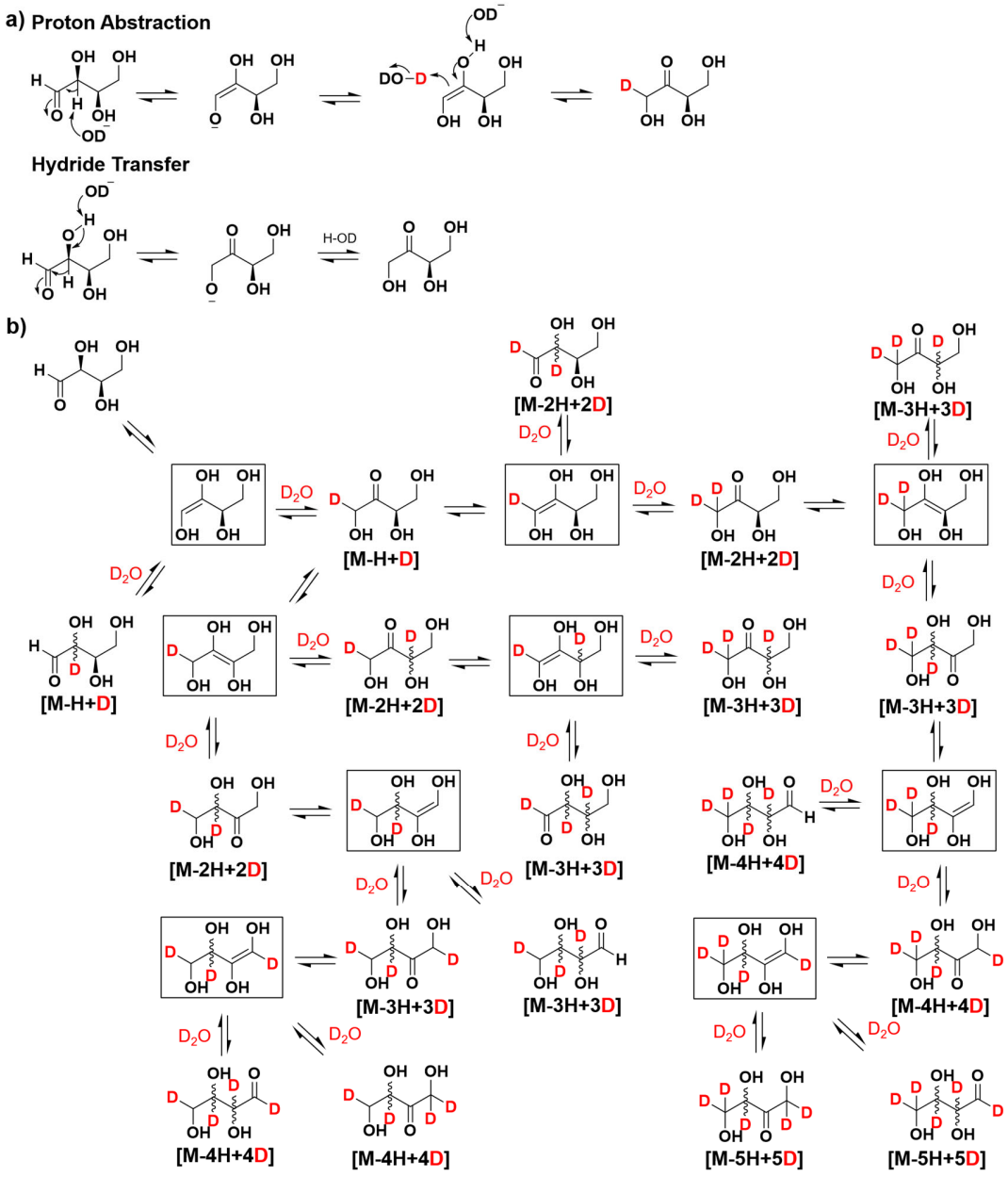

Scheme S2. a) Two mechanistic pathways of carbonyl migration: enediol(ate) and 1,2-hydride shift. Note that deuterium incorporation would not take place via intramolecular hydride transfer. b) The potential process of deuterium incorporation into the threose carbon chain via carbonyl migration by deprotonation of the alpha-carbon followed by formation of an enediol (enediolate) intermediate that is consistent with the MS data, which reveals that as carbonyl migration progresses, deuterium incorporation increases.

6.Table of peak intensity detected in ^{13}C NMR spectra

6.1 D-[1-^{13}C]-Erythrose

6.1.1 pH 8.5, 160 mM $NaHCO_3$, 25 °C

Table S1. The peak intensity of compound **2**–**15** detected in the ^{13}C NMR spectra of 80 mM D-[1-^{13}C]-erythrose in 160 mM $NaHCO_3$ at pH 8.5 at 25 °C (shown in **Figure 1**).

	Peak/ ppm																
No. T/ h	**G1**	**11**	**6**	**11[a]**	**G2**	**5**	**12**	**14**, **15**	**2**	**8**	**3**	**9**	**4**	**10**	**F**	**Others**	**Sum**
	60.4	61.6	62.0	62.4	63.2	65.0	69.0-72.3	69.0-75.5	88.5	88.9	94.5	95.7	100.2	101.2	170.1		
0	0.00	0.01	0.00	0.00	0.03	0.74	0.24	0.00	1.95	0.01	4.47	0.00	11.22	0.00	0.03	0.64	19.39
1	0.00	0.02	0.05	0.00	0.10	1.64	0.22	0.08	1.93	0.01	4.62	0.00	10.89	0.05	0.04	0.88	20.49
2	0.00	0.01	0.08	0.00	0.15	2.33	0.17	0.12	1.74	0.01	4.17	0.00	9.79	0.09	0.05	0.77	19.31
3	0.00	0.01	0.13	0.00	0.18	3.02	0.15	0.19	1.62	0.01	4.01	0.00	9.26	0.11	0.05	0.67	19.18
4	0.00	0.01	0.19	0.00	0.22	3.62	0.17	0.22	1.56	0.02	3.68	0.06	8.74	0.16	0.05	0.53	19.03
5	0.00	0.01	0.27	0.00	0.25	4.13	0.13	0.34	1.45	0.02	3.20	0.23	8.19	0.21	0.06	1.13	18.94
6	0.00	0.01	0.34	0.00	0.38	4.73	0.14	0.39	1.41	0.03	3.07	0.25	7.80	0.24	0.05	1.00	19.24
7	0.00	0.01	0.43	0.00	0.32	5.17	0.12	0.48	1.34	0.04	2.90	0.27	7.56	0.27	0.05	0.95	19.27
8	0.00	0.01	0.51	0.00	0.34	5.54	0.09	0.55	1.27	0.04	2.73	0.26	7.01	0.30	0.05	0.97	18.97
9	0.00	0.01	0.60	0.00	0.37	5.86	0.14	0.61	1.20	0.04	2.66	0.26	6.70	0.32	0.06	0.98	19.16
10	0.00	0.01	0.68	0.00	0.37	6.14	0.11	0.62	1.14	0.05	2.40	0.30	6.38	0.34	0.06	1.06	18.90
11	0.00	0.01	0.78	0.00	0.40	6.48	0.12	0.72	1.10	0.05	2.26	0.35	6.15	0.37	0.05	1.16	19.10
12	0.00	0.01	0.87	0.00	0.39	6.69	0.10	0.82	1.02	0.05	2.17	0.41	5.79	0.39	0.06	1.22	19.10
13	0.00	0.01	0.98	0.00	0.42	6.95	0.14	0.81	0.99	0.06	2.08	0.44	5.48	0.45	0.06	1.22	19.04
14	0.00	0.01	1.06	0.00	0.43	6.91	0.12	0.86	0.91	0.07	2.00	0.50	5.07	0.47	0.05	0.86	18.75
15	0.00	0.01	1.14	0.00	0.45	7.18	0.13	0.94	0.88	0.08	1.88	0.49	4.96	0.53	0.06	0.95	19.06
16	0.00	0.02	1.19	0.00	0.45	7.19	0.13	0.96	0.83	0.08	1.74	0.52	4.65	0.55	0.06	1.17	18.86
67	0.03	0.08	3.18	0.00	0.50	7.54	0.48	2.12	0.35	0.18	0.84	0.77	2.01	0.99	0.07	1.23	20.00
89	0.04	0.09	3.54	0.03	0.48	7.11	0.72	2.70	0.28	0.20	0.61	0.78	1.61	1.09	0.13	1.18	20.46
109	0.05	0.09	3.81	0.03	0.38	6.36	0.80	2.70	0.23	0.19	0.43	0.72	1.27	1.08	0.16	1.76	19.83

2: D-[1-^{13}C]-erythrose hydrate; **3**: α-D-[1-^{13}C]-erythrofuranose; **4**: β-D-[1-^{13}C]-erythrofuranose; **5**: R-[1-^{13}C]-erythrulose; **6**: *rac*-[4-^{13}C]-erythrulose; **8**: D-[1-^{13}C]-threose hydrate; **9**: β-D-[1-^{13}C]-threofuranose; **10**: α-D-[1-^{13}C]-threofuranose; **11**: *rac*-[4-^{13}C]-tetrose hydrate; **12**: *rac*-[4-^{13}C]-tetrose furanose; **14**, **15**: diastereomeric C8 species; **G1**: glycolate; **G2**: glycerate; **F**: formate; **Others**: unsigned peaks; **Sum**: total intensity observed in each spectrum.

6.1.2 pH 5, 160 mM acetate, 40 °C

Table S2. The peak intensity of compound **1**–**6** detected in the ^{13}C NMR spectra of 80 mM D-[1-^{13}C]-erythrose in 160 mM acetate buffer at pH 5 at 40 °C (shown in **Figure S1**).

	Peak/ ppm							
No.	**5**	**2**	**3**	**4**	**F**[a]	**1**[a]	**Others**	**Sum**
T/ h	65.0	88.6	94.6	100.3	169.6	203.6		
0	0.01	2.90	7.99	17.95	0.03	0.01	2.33	31.93
1	0.02	2.90	7.90	17.76	0.01	0.03	1.99	31.26
2	0.02	2.80	7.60	17.19	0.02	0.02	1.59	29.92
3	0.02	2.92	7.90	17.89	0.02	0.02	1.51	30.93
4	0.03	3.02	8.15	18.46	0.03	0.03	1.40	31.82
5	0.03	2.87	7.80	17.57	0.03	0.02	1.51	30.52
6	0.03	2.96	8.05	18.07	0.04	0.05	1.55	31.40
7	0.02	2.85	7.73	17.51	0.04	0.02	1.71	30.51
8	0.02	2.97	7.88	17.80	0.03	0.03	1.50	30.87
9	0.03	3.02	8.22	18.89	0.06	0.02	1.34	32.30
10	0.03	2.92	7.90	17.82	0.04	0.02	1.59	31.03
11	0.03	2.88	7.83	17.67	0.05	0.04	1.54	30.68
12	0.03	3.13	8.50	19.12	0.06	0.02	1.59	33.12
13	0.04	2.92	7.87	17.83	0.05	0.03	1.64	31.03
21	0.04	2.94	7.89	17.83	0.08	0.03	2.06	31.49
70	0.09	2.78	7.47	16.89	0.27	0.02	2.05	30.22
100	0.12	3.15	8.48	19.05	0.41	0.02	2.56	34.52

[a] D-[1-^{13}C]-Erythrose aldose; **F**: Formate; **Others**: Unsigned peaks; **Sum**: Total intensity observed in each spectrum.

6.1.3 pH 7, 160 mM NaH_2PO_4, 40 °C

Table S3. The peak intensity of compound **1**–**15** detected in the ^{13}C NMR spectra of 80 mM D-[1-^{13}C]-erythrose in 160 mM NaH_2PO_4 buffer at pH 7 at 40 °C (shown in **Figure S2**).

	Peak/ ppm																	
No.	**G1**	**11**	**6**	**11**	**G2**	**5**	**12**	**14**, **15**	**2**	**8**	**3**	**9**	**4**	**10**	**F**	**1**[a]		
T/ h							69.5-										**Others**	**Sum**
	60.4	61.7	62.0	62.4	63.3	65.0	72.0	69.0-75.5	88.6	89.0	94.6	95.7	100.3	101.2	170.0	203.9		
0	0.00	0.03	0.00	0.00	0.00	0.15	0.41	0.00	2.92	0.00	7.72	0.00	17.23	0.00	0.02	0.22	1.35	30.05
1	0.00	0.02	0.00	0.00	0.03	0.54	0.37	0.00	2.78	0.00	7.26	0.00	16.00	0.00	0.01	0.22	1.72	28.95
2	0.00	0.02	0.01	0.00	0.05	0.86	0.39	0.00	2.76	0.00	7.32	0.00	15.96	0.03	0.03	0.21	1.56	29.20
3	0.00	0.03	0.01	0.00	0.06	1.32	0.41	0.00	2.70	0.00	7.10	0.00	15.64	0.04	0.05	0.26	1.35	28.97
4	0.00	0.01	0.04	0.00	0.09	1.88	0.37	0.06	2.66	0.00	7.08	0.04	15.57	0.04	0.04	0.30	1.33	29.51
5	0.00	0.02	0.06	0.00	0.11	2.40	0.35	0.06	2.66	0.01	7.04	0.04	15.51	0.03	0.04	0.22	1.56	30.11
6	0.00	0.02	0.07	0.00	0.14	2.84	0.36	0.06	2.50	0.01	6.60	0.04	14.72	0.05	0.06	0.23	1.30	29.00
7	0.00	0.03	0.11	0.00	0.17	3.45	0.37	0.10	2.51	0.01	6.66	0.06	14.67	0.08	0.08	0.19	1.46	29.95
8	0.00	0.03	0.12	0.00	0.20	3.83	0.37	0.14	2.41	0.01	6.37	0.06	14.04	0.10	0.07	0.13	1.23	29.11
9	0.00	0.04	0.15	0.00	0.21	4.12	0.37	0.16	2.29	0.02	6.06	0.08	13.56	0.11	0.05	0.27	0.78	28.27
10	0.00	0.03	0.20	0.00	0.23	4.65	0.35	0.14	2.22	0.01	5.89	0.08	13.23	0.13	0.06	0.21	0.88	28.31
11	0.00	0.03	0.23	0.00	0.23	5.04	0.34	0.20	2.24	0.02	5.87	0.10	13.25	0.11	0.08	0.16	1.04	28.94
12	0.00	0.03	0.26	0.00	0.29	5.45	0.33	0.22	2.19	0.02	5.83	0.10	13.06	0.15	0.08	0.18	0.76	28.95
13	0.00	0.03	0.27	0.00	0.30	5.72	0.35	0.22	2.20	0.02	5.82	0.12	13.00	0.16	0.08	0.18	0.86	29.33
47	0.09	0.05	1.96	0.06	0.65	12.26	0.53	0.92	1.00	0.13	2.79	0.53	6.31	0.72	0.40	0.00	1.86	30.17
72	0.20	0.08	2.35	0.06	0.53	9.87	0.68	0.90	0.52	0.13	1.52	0.61	3.33	0.82	0.59	0.00	1.52	23.51
95	0.31	0.10	3.50	0.09	0.63	10.94	1.08	1.12	0.45	0.19	1.20	0.81	2.83	1.08	0.79	0.00	2.32	27.13
117	0.42	0.11	4.01	0.12	0.65	10.18	1.40	1.36	0.35	0.21	0.92	0.90	2.14	1.21	0.92	0.00	3.08	27.56

[a] D-[1-^{13}C]-Erythrose aldose; **G1**: Glycolate; **G2**: Glycerate; **F**: Formate; **Others**: Unsigned peaks; **Sum**: Total intensity observed in each spectrum.

6.1.4 pH 8.5, 160 mM $NaHCO_3$, 40 °C

Table S4. The peak intensity of compound **2**–**15** detected in the ^{13}C NMR spectra of 80 mM D-[1-^{13}C]-erythrose in 160 mM $NaHCO_3$ buffer at pH 8.5 at 40 °C (shown in **Figure S3**).

	Peak/ ppm																
No.	**G1**	**11**	**6**	**11**	**G2**	**5**	**12**	**14**, **15**	**2**	**8**	**3**	**9**	**4**	**10**	**F**	**Others**	**Sum**
T/h	60.4	61.7	62.0	62.4	63.3	65.0	69.0-72.3	69.0-75.5	88.6	89.0	94.4	95.6	100.3	101.2	170.0		
0	0.00	0.02	0.07	0.00	0.12	2.64	0.24	0.28	2.43	0.00	5.02	0.00	15.91	0.00	0.05	0.55	27.33
1	0.00	0.01	0.71	0.00	0.36	8.11	0.21	0.84	1.71	0.05	4.12	0.00	10.48	0.38	0.07	0.87	27.92
2	0.00	0.02	1.26	0.00	0.48	10.27	0.17	1.24	1.46	0.07	3.68	0.00	9.44	0.88	0.08	0.00	28.95
3	0.01	0.02	1.74	0.00	0.53	11.08	0.22	1.56	1.19	0.09	2.60	0.50	7.66	0.95	0.08	0.04	28.26
4	0.01	0.03	2.29	0.01	0.56	11.75	0.27	1.94	0.99	0.11	1.93	0.70	6.68	1.06	0.08	0.10	28.50
5	0.01	0.03	2.81	0.02	0.57	12.34	0.28	2.08	0.86	0.13	1.40	1.40	5.95	1.19	0.08	0.00	29.06
6	0.03	0.07	3.21	0.02	0.60	11.69	0.32	2.34	0.69	0.15	1.17	1.69	4.68	1.21	0.08	0.01	27.93
7	0.03	0.04	3.51	0.02	0.59	11.94	0.47	2.62	0.63	0.16	1.00	1.75	4.47	1.29	0.09	0.27	28.85
8	0.03	0.05	3.90	0.02	0.58	11.62	0.49	2.76	0.53	0.16	0.77	1.73	3.97	1.33	0.09	0.11	28.11
9	0.04	0.08	4.21	0.03	0.58	11.55	0.64	2.98	0.46	0.18	0.65	1.71	3.82	1.41	0.10	0.23	28.63
10	0.04	0.08	4.59	0.03	0.60	11.46	0.75	3.12	0.42	0.18	0.58	1.79	3.31	1.27	0.09	1.01	29.28
11	0.05	0.10	4.64	0.04	0.60	10.77	0.76	3.04	0.36	0.19	0.44	1.80	2.87	1.38	0.09	1.24	28.35
12	0.06	0.14	5.15	0.05	0.60	10.61	0.84	3.66	0.32	0.20	0.38	1.92	2.37	1.43	0.09	1.58	29.15

G1: Glycolate; **G2**: Glycerate; **F**: Formate; **Others**: Unsigned peaks; **Sum**: Total intensity observed in each spectrum.

6.1.5 pH 10, 160 mM $NaHCO_3$, 40 °C

Table S5. The peak intensity of compound **2-15** detected in the ^{13}C NMR spectra of 80 mM D-[1-^{13}C]-erythrose in 160 mM $NaHCO_3$ buffer at pH 10 at 40 °C (shown in **Figure S4**).

	Peak/ ppm										
No.	**G1**	**6**	**G2**	**5**	**14**, **15**	**2**	**8**	**3**, **4**, **9**, **10**[a]	**F**	**Others**	**Sum**
T/ h	60.4	62.0	63.3	65.0	69.5-76.0	88.7	89.0	95.4-105.2	170.0		
0	0.00	0.15	0.14	3.38	1.28	2.50	0.00	22.72	0.09	0.36	30.62
1	0.00	1.56	0.45	7.70	7.16	1.02	0.05	10.11	0.08	0.36	28.49
2	0.04	2.67	0.46	6.91	12.18	0.41	0.08	4.78	0.21	1.52	29.22
3	0.08	3.02	0.36	5.85	12.94	0.23	0.13	3.50	0.27	3.49	29.79
4	0.10	3.27	0.44	5.09	14.50	0.15	0.09	2.61	0.42	4.48	31.05
5	0.13	3.31	0.48	4.15	14.22	0.10	0.09	2.16	0.44	5.28	30.23
6	0.16	2.91	0.47	3.58	15.54	0.07	0.08	1.98	0.47	6.85	31.95
7	0.16	2.61	0.49	3.00	15.64	0.05	0.07	1.47	0.47	6.65	30.45
8	0.17	2.32	0.44	2.31	15.64	0.02	0.05	1.21	0.53	7.15	29.67
9	0.23	2.28	0.55	2.13	15.84	0.02	0.04	1.24	0.57	8.65	31.32
10	0.24	2.19	0.52	1.91	15.94	0.03	0.04	1.15	0.56	8.55	30.89
11	0.24	1.93	0.54	1.61	15.30	0.02	0.04	1.02	0.59	8.57	29.62
12	0.25	1.71	0.54	1.36	11.66	0.01	0.02	0.63	0.57	11.36	25.89
13	0.25	1.69	0.61	1.37	14.96	0.01	0.02	0.76	0.60	9.43	29.45
14	0.27	1.63	0.63	1.25	14.48	0.00	0.03	0.82	0.64	9.92	29.40
24	0.35	0.89	0.44	0.72	15.56	0.01	0.01	0.66	0.43	13.07	31.79
48	0.37	0.36	0.48	0.25	9.60	0.00	0.00	0.37	0.56	11.64	23.26

[a] Because the signals of **3**, **4**, **9**, **10** are broad and difficult to identify separately, the intensity of these peaks are combined; **G1**: glycolate; **G2**: glycerate; **F**: Formate; **Others**: Unsigned peaks; **Sum**: Total intensity observed in each spectrum.

6.1.6 pH 7, 480 mM NaH_2PO_4, 40 °C

Table S6. The peak intensity of compound **1-15** detected in the ^{13}C NMR spectra of 80 mM D-[1-^{13}C]-erythrose in 480 mM phosphate buffer at pH 7 at 40 °C (shown in **Figure S5**).

	Peak/ ppm																
No.	**G1**	**11**	**6**	**11**	**G2**	**5**	**12**	**14, 15**	**2**	**8**	**3**	**9**	**4**	**10**	**F**		
T/ h	60.4	61.7	62.0	62.4	63.3	65.0	69.0-72.3	69.5-75.5	88.6	88.9	94.6	95.7	100.3	101.2	170.1	**Others**	**Sum**
0	0.00	0.05	0.07	0.00	0.00	0.49	0.71	0.00	5.43	0.00	14.10	0.00	28.86	0.00	0.04	3.30	53.44
1	0.00	0.07	0.05	0.00	0.13	2.71	0.54	0.00	5.69	0.00	14.60	0.04	30.14	0.08	0.10	3.14	57.84
2	0.00	0.06	0.15	0.00	0.25	4.71	0.54	0.07	4.74	0.00	11.99	0.10	24.85	0.20	0.10	2.21	50.38
3	0.00	0.06	0.25	0.00	0.39	6.88	0.61	0.12	4.82	0.02	12.46	0.11	26.21	0.16	0.09	2.53	54.71
4	0.00	0.06	0.39	0.00	0.54	9.71	0.66	0.12	4.89	0.04	12.56	0.15	26.24	0.27	0.10	2.58	58.31
5	0.00	0.06	0.55	0.00	0.58	10.75	0.48	0.24	4.34	0.04	11.29	0.22	23.31	0.30	0.14	2.60	54.90
6	0.00	0.05	0.69	0.00	0.67	12.15	0.50	0.28	4.03	0.06	10.26	0.21	21.82	0.42	0.09	1.70	52.93
7	0.00	0.05	0.86	0.00	0.71	13.47	0.48	0.38	3.87	0.06	10.02	0.25	20.45	0.42	0.10	2.22	53.34
8	0.00	0.04	1.11	0.00	0.81	15.79	0.51	0.52	3.91	0.06	10.11	0.35	21.15	0.48	0.12	1.46	56.42
9	0.00	0.05	1.63	0.00	1.08	20.53	0.58	0.56	4.41	0.12	11.53	0.46	23.98	0.69	0.16	1.92	67.70
10	0.00	0.04	1.68	0.00	0.98	19.32	0.51	0.60	3.87	0.09	9.82	0.47	20.77	0.63	0.11	2.05	60.94
11	0.00	0.04	1.84	0.00	1.05	19.84	0.51	0.60	3.58	0.11	9.21	0.57	19.54	0.82	0.12	1.11	58.94
13	0.00	0.05	2.22	0.00	1.02	20.18	0.47	0.66	3.03	0.15	7.96	0.58	16.83	0.89	0.14	1.55	55.73
18	0.00	0.05	3.74	0.00	1.38	25.77	0.64	0.93	2.81	0.22	7.43	1.03	15.50	1.35	0.18	1.62	62.65
21	0.02	0.05	4.00	0.00	1.23	24.73	0.71	1.02	2.32	0.24	6.13	1.01	12.99	1.43	0.18	1.53	57.57
48	0.21	0.17	8.89	0.00	1.38	25.07	1.71	1.38	0.97	0.50	2.55	1.92	5.53	2.63	0.57	4.02	57.29
67	0.45	0.24	13.47	0.14	1.49	28.16	2.93	1.86	0.81	0.68	2.27	2.76	4.90	3.80	1.08	7.71	72.30
93	0.75	0.29	12.89	0.15	1.04	19.79	3.75	1.78	0.48	0.61	1.24	2.29	2.70	3.09	1.26	8.65	60.01
127	1.09	0.33	13.58	0.23	1.11	17.86	4.00	2.12	0.38	0.55	1.06	2.15	2.22	2.97	1.52	10.68	60.76
144	1.45	0.33	13.08	0.16	1.01	15.42	4.46	1.98	0.32	0.52	0.89	2.06	1.90	2.64	1.91	13.23	59.91

G1: glycolate; **G2**: glycerate; **F**: Formate; **Others**: Unsigned peaks; **Sum**: Total intensity observed in each spectrum.

6.1.7 pH 7, 160 mM cacodylate, 40 °C

Table S7. The peak intensity of compound **1-15** detected in the ^{13}C NMR spectra of D-[1-^{13}C]-erythrose with 160 mM cacodylate buffer at pH 7 at 40 °C (shown in **Figure S6**).

	Peak/ ppm																	
No.	**G1**	**11**	**6**	**11**	**G2**	**5**	**12**	**14, 15**	**2**	**8**	**3**	**9**	**4**	**10**	**F**	**1[a]**		
T/ h	60.4	61.7	62.0	62.4	63.3	65.0	69.0-72.3	69.5-75.5	88.7	89.0	94.6	95.6	100.3	101.2	170.0	203.7	**Others**	**Sum**
0	0.00	0.00	0.00	0.00	0.00	0.05	0.41	0.00	2.94	0.00	8.10	0.00	18.35	0.00	0.02	0.46	1.60	31.93
1	0.00	0.00	0.00	0.00	0.00	0.15	0.42	0.00	2.95	0.00	8.12	0.00	18.41	0.00	0.12	0.41	1.73	32.31
3	0.00	0.00	0.00	0.00	0.02	0.44	0.40	0.00	2.82	0.00	7.65	0.00	17.65	0.00	0.20	0.27	2.02	31.47
5	0.00	0.00	0.00	0.00	0.04	0.66	0.32	0.00	2.79	0.00	7.52	0.00	17.16	0.00	0.38	0.37	1.84	31.08
6	0.00	0.00	0.00	0.00	0.03	1.04	0.33	0.00	2.86	0.00	7.48	0.00	17.08	0.00	0.42	0.31	1.87	31.42
7	0.00	0.00	0.00	0.00	0.05	1.34	0.35	0.00	2.63	0.00	7.25	0.01	16.36	0.02	0.44	0.54	1.66	30.65
8	0.00	0.00	0.02	0.00	0.07	1.62	0.36	0.00	2.60	0.00	6.89	0.02	15.68	0.04	0.44	0.41	1.56	29.71
9	0.00	0.00	0.04	0.00	0.09	2.01	0.35	0.00	2.57	0.00	6.95	0.04	15.81	0.05	0.50	0.35	1.61	30.37
10	0.00	0.00	0.05	0.00	0.09	2.32	0.36	0.00	2.64	0.00	7.12	0.05	16.20	0.06	0.59	0.36	1.64	31.48
11	0.00	0.00	0.05	0.00	0.13	2.49	0.35	0.00	2.51	0.00	6.75	0.03	15.30	0.08	0.60	0.37	1.93	30.59
12	0.00	0.00	0.07	0.00	0.15	2.92	0.39	0.00	2.58	0.00	7.07	0.04	16.06	0.07	0.63	0.34	1.60	31.92
13	0.00	0.00	0.08	0.00	0.14	3.06	0.38	0.00	2.43	0.01	6.71	0.04	15.33	0.07	0.66	0.41	1.46	30.78
14	0.00	0.00	0.10	0.00	0.15	3.34	0.32	0.00	2.36	0.01	6.50	0.03	14.67	0.10	0.68	0.31	1.82	30.39
15	0.00	0.00	0.11	0.00	0.15	3.47	0.35	0.00	2.23	0.01	6.25	0.07	14.09	0.07	0.68	0.30	1.32	29.10
28	0.08	0.01	0.22	0.00	0.20	4.09	0.28	0.32	1.89	0.03	5.35	0.11	12.18	0.13	1.78	0.22	2.28	29.09
49	0.16	0.06	0.50	0.09	0.31	5.78	0.27	0.50	1.33	0.05	3.80	0.26	8.74	0.25	2.59	0.22	2.41	27.07
73	0.22	0.05	0.77	0.11	0.35	6.97	0.26	0.64	1.08	0.07	3.04	0.27	7.06	0.39	3.04	0.24	2.40	26.63
122	0.24	0.04	1.10	0.04	0.40	6.87	0.26	0.50	0.71	0.09	1.84	0.38	4.54	0.51	3.14	0.08	3.16	23.62
145	0.27	0.08	1.52	0.12	0.42	8.08	0.31	0.82	0.64	0.11	1.81	0.48	4.27	0.65	3.25	0.08	3.32	25.84

[a] D-[1-^{13}C]-Erythrose aldose; **G1**: glycolate; **G2**: glycerate; **F**: Formate; **Others**: Unsigned peaks; **Sum**: Total intensity observed in each spectrum.

6.2 D-[4-^{13}C]-Erythrose, pH 8.5, 250 mM $NaHCO_3$, 40 °C

Table S8. The peak intensity of compound **2′-12′** detected in the ^{13}C NMR spectra of D-[4-^{13}C]-erythrose at pH 8.5 at 40 °C as shown in **Figure S7**.

	Peak/ ppm												
No.	**2′**	**5′**	**8′**	**G2**	**6′**	**9′**	**3′** and **4′**	**10′**	**11′**	**12′**	**F**	**Others**	**Sum**
T/h	61.7	62.0	62.4	63.3	65.0	69.4	70.1	72.0	88.4-89.2	94.5-101.8	170.0		
0	3.49	0.57	0.00	0.02	0.00	0.00	29.32	0.13	0.02	0.14	0.00	1.08	34.77
1	2.84	4.18	0.00	0.20	0.13	0.00	23.61	0.40	0.02	0.13	0.00	1.95	33.46
3	1.35	5.01	0.00	0.26	0.41	0.00	12.31	0.26	0.00	0.00	0.00	2.33	21.93
6	1.44	9.85	0.06	0.83	1.33	0.49	12.16	0.54	0.00	0.00	0.02	6.01	32.73
8	1.07	10.50	0.07	1.22	2.06	0.72	8.25	0.61	0.01	0.11	0.07	7.48	32.17
10	1.00	10.88	0.14	1.82	2.69	0.93	6.64	0.94	0.02	0.30	0.12	9.56	35.04
12	0.88	10.77	0.14	2.32	3.14	1.05	5.33	1.05	0.03	0.37	0.18	9.98	35.24

[a] **2′**: D-[4-^{13}C]-erythrose hydrate; **3′**: α-D-[4-^{13}C]-erythrofuranose; **4′**: β-D-[4-^{13}C]-erythrofuranose; **5′**: R-[4-^{13}C]-erythrulose; **6′**: *rac*-[1-^{13}C]-erythrulose; **8′**: D-[4-^{13}C]-threose hydrate; **9′**: β-D-[4-^{13}C]-threofuranose; **10′**: α-D-[4-^{13}C]-threofuranose; **11′**: *rac*-[1-^{13}C]-tetrose hydrate; **12′**: *rac*-[1-^{13}C]-tetrose furanose; **G1**: glycerate; **F**: formate; **Others**: unsigned peaks; **Sum**: total intensity observed in each spectrum.

6.3 D-[1-^{13}C]-Threose, pH 8.5, 160 mM $NaHCO_3$, 40 °C

Table S9. The peak intensity of compound **1-15** detected in the ^{13}C NMR spectra of D-[1-^{13}C]-threose at pH 8.5 at 40 °C as shown in **Figure S9**.

	Peak/ppm																
No.	**G1**	**11**	**6**	**11**	**G2**	**5**	**12**	**14**, **15**	**2**	**8**	**3**	**9**	**4**	**10**	**F**	**Others**	**Sum**
T/h	60.4	61.7	62.0	62.4	63.3	65.0	71.9	66.5-76.0	88.7	89.0	94.6	95.7	100.2	101.2	170.0		
0	0.00	0.00	0.02	0.00	0.01	0.25	0.11	0.00	0.00	2.69	0.00	10.80	0.00	14.64	0.02	1.06	29.60
1	0.00	0.00	0.04	0.00	0.04	1.10	0.10	0.00	0.00	2.45	0.00	9.80	0.00	13.65	0.04	1.07	28.29
2	0.00	0.00	0.10	0.00	0.11	2.08	0.13	0.18	0.00	2.45	0.00	10.09	0.00	13.68	0.07	1.17	30.06
3	0.00	0.00	0.18	0.00	0.13	2.80	0.12	0.36	0.02	2.28	0.00	9.16	0.23	12.77	0.13	1.23	29.37
4	0.00	0.00	0.27	0.00	0.16	3.20	0.11	0.56	0.02	2.00	0.00	8.22	0.25	11.42	0.17	1.07	27.49
5	0.01	0.00	0.34	0.00	0.18	3.89	0.11	0.89	0.03	2.03	0.00	8.04	0.31	11.29	0.22	1.24	28.57
6	0.01	0.00	0.44	0.00	0.22	4.33	0.11	1.12	0.04	1.85	0.00	8.25	0.46	10.68	0.28	1.18	28.96
7	0.02	0.00	0.51	0.00	0.23	4.63	0.10	1.20	0.05	1.77	0.00	7.34	0.41	10.34	0.35	1.06	27.92
8	0.02	0.00	0.63	0.00	0.27	5.03	0.13	1.44	0.05	1.73	0.00	7.53	0.52	10.18	0.39	1.05	28.90
9	0.03	0.00	0.69	0.00	0.29	5.06	0.10	1.50	0.04	1.6	0.00	6.92	0.41	9.40	0.42	1.44	27.97
10	0.03	0.00	0.81	0.00	0.30	5.54	0.11	1.76	0.05	1.61	0.00	6.99	0.41	9.66	0.50	1.22	29.04
11	0.04	0.00	0.88	0.00	0.32	5.61	0.10	1.86	0.07	1.54	0.00	6.47	0.41	9.02	0.50	1.91	28.40
12	0.04	0.00	0.94	0.01	0.34	5.72	0.13	2.09	0.06	1.51	0.00	6.41	0.46	8.84	0.56	1.63	29.39
13	0.05	0.01	0.95	0.01	0.31	5.45	0.11	2.06	0.05	1.34	0.00	5.86	0.48	7.92	0.54	1.37	26.64

G1: glycolate; **G2**: glycerate; **F**: Formate; **Others**: Unsigned peaks; **Sum**: Total intensity observed in each spectrum.